



International  
**JOURNAL** of  
**SEWC**

— Structural Engineers World Congress —

ISSN 2249-183X



9 772249 183004



## President's Message

Greetings and welcome to you all from SEWC on the occasion of the release of another edition of the SEWC Journal. Also let me express my best wishes for a prosperous and peaceful 2019.

I am happy that our journal publications are acknowledged well in the field of structural engineering. Thanks to our Editorial team. This encouragement of-course makes us to work harder so as to maintain the quality of publication still better.

As I indicated earlier it will be our endeavour to make the SEWC journal as a source of information related to civil engineering and especially structural engineering with quality technical contents and I must say that it is gaining momentum. I hope readers of SEWC Journal will gain through reading the articles published in the Journal from time to time.

May I take this opportunity of informing you that the 7th International Congress of Structural Engineering World Congress in Istanbul, Turkey is being organized by SEWC Turkey Group during April 24th - 26th, 2019 under the Chairmanship of Prof. Goren Arun. Preparations to conduct this prestigious Congress is in the advanced stage and I am sure of the success. SEWC extends a welcome to all to attend the symposium in Istanbul.

Wish you a very Happy & Prosperous new year.

### **R. SUNDARAM**

President – Structural Engineers World Congress, Worldwide

Member – Advisory Board, International Association for Shell and Spatial Structures [IASS].



R. SUNDARAM



## Editorial

As the President, SEWC has said the journal keeps its priority on quality and originality of the papers published. The readers till now would have observed that the papers from the previous conferences would be selected based on merit and published in the subsequent issues of the journal. It is a matter of pride to share with the readers that the most of the papers in all the previous SEWC conferences were always of very good quality. It was very difficult to choose only a few like 6 or 7 out of so many good papers. That evidently proves that the structural engineering community is very conscious of the quality of the papers they write as much and no less than the quality of design and construction they do. I believe that the SEWC journal is doing its contribution by disseminating the wisdom of the community to a wider audience.

**B K Raghu Prasad**

Editor-in-Chief



## Obituary

With profound grief we inform the sad demise of our beloved Prof. Roland L Sharpe, Co-Founder and Past President of SEWC Inc. recently. He had a long and successful career in many capacities whichever organizations/associations with which he was involved. He was a distinguished Member, ASCE(USA) and Honorary Member of five other national and international professional organizations. He was Author/co-author of over 200 technical papers, books, and reports. He had a passion for structural engineering. His demise leaves a void in the structural engineering fraternity and we salute his immense contribution to structural engineering. We fondly remember his services and his ever positive attitude. On behalf of the SEWC our deepest condolences to his family and friends for this irreparable loss. He remains very much in our thoughts. May his soul be blessed with eternal peace.



Prof. Roland L Sharpe





## SEWC Board Members

---

- |   |   |
|---|---|
| 1 Mr. R. Sundaram, India, President                   | 10 Prof. SeungDeog Kim, South Korea         |
| 2 Prof. Narendra K Srivastava, Canada, Vice President | 11 Prof. Juan Gerardo Oliva Salinas, Mexico |
| 3 Prof. Toshio Okoshi, Japan, Vice President          | 12 Prof. Gorun Arun, Turkey                 |
| 4 Prof. Ing. Enzo Siviero, Italy, Vice President      | 13 Er. Lim Peng Hong, Singapore             |
| 5 Dr. Gian Carlo Giuliani, Italy                      | 14 Er. Abhishek Murthy, Singapore           |
| 6 Dr. James R. Cagley, USA                            | 15 Mr. Knut Stockhusen, Germany             |
| 7 Prof. A. H-S. Ang, USA                              | 16 Prof. Akira Wada, Japan                  |
| 8 Prof. Sung Pil Chang, South Korea                   | 17 Prof. Romuald Tarczewski, Poland         |
| 9 Prof. Ding Jiemin, China                            |   |



# Content

---

- 13**    **Model Updating of A Super Tall Building in Shanghai with Ambient Vibration Test Data**  
Yuxin Pan, Carlos E. Ventura, Haibei Xiong, Fengliang Zhang
  
- 18**    **Analysis of the concept: Seismic Resilience**  
Juan Carlos Flores, Mabel Mendoza, Hugo Castellanos
  
- 24**    **Spline arch – A pneumatic Chamber system applied in a temporary membrane structure**  
Juan Jose Ramirez
  
- 27**    **Expanded Applications of High Performance Fiber Rope As Building Structural Members**  
Natsuki Yasui, Kaidoh Yamaguchi, Osamu Takahashi, Kaori Tsukano, Yoshinori Tateoka
  
- 33**    **Structural Design of a Seismic Isolated Building in Matsumoto City, Japan**  
Yuki Nagai, Toshiaki Kimura, Musturo Sasaki
  
- 39**    **Pedestrianisation of Meenakshi Temple Surrounds**  
Ar. ValliappanRamanathan
  
- 46**    **Construction wastes used for manufacturing RA-bricks**  
Armando Aguilar-Penagos, Alberto López, José Gómez-Soberón, Neftalí Rojas-Valencia
  
- 51**    **Sustainable Concrete Solutions for Buildings in the UK**  
Costas Georgopoulos, Andrew Minson
  
- 57**    **NEWS**



# Model Updating of A Super Tall Building in Shanghai with Ambient Vibration Test Data

**Yuxin Pan<sup>1\*</sup>, Carlos E. Ventura<sup>2</sup>, Haibei Xiong<sup>3</sup>, Fengliang Zhang<sup>4</sup>**

<sup>1</sup> Department of Civil Engineering, University of British Columbia, Canada

<sup>2</sup> Department of Civil Engineering, University of British Columbia, Canada

<sup>3</sup> College of Civil Engineering, Tongji University, China

<sup>4</sup> College of Civil Engineering, Tongji University, China

**Abstract:** The Shanghai Tower is the tallest structure in China and one of the super tall buildings in the world. The building stands approximately 632 meters and has 128 stories. On May 8th, 2015, an ambient vibration test was performed on this building in its final stage of construction by a collaborative team from the University of British Columbia and Tongji University. The first nine modes of vibration and the associated damping ratios were determined below 1Hz by using the operational modal analysis. A simple and efficient lumped-mass stick model based on the macro beam theory was developed in SAP2000 as the baseline model for updating. By performing the sensitivity analysis, several sets of parameters were selected and then modified with an automated updating procedure. An average of 4.4% difference between natural frequencies of all nine modes was obtained, and the updated properties of FE model successfully maximize the modal assurance criterion (MAC) and minimize the discrepancies of periods between real structure and numerical model. The updated new FE model is now reliable for wide range of applications in the area of seismic performance, long term health monitoring and risk assessment.

## 1. INTRODUCTION

In recent years, to meet both economic and social needs, the design and construction of super tall buildings is a merging topic in China. Since 2010, more than 50 high-rise buildings in China over 300 m have been either constructed or proposed. Significant example is the Shanghai Tower, which was initially designed in 2006 and just starts its trial operation in January 2017 in Lujiazui District, Shanghai, China. As the tallest structure in China, Shanghai Tower has 127 stories above the ground with a total height of 632 m, as seen in Fig. 1. A triangular outer facade encloses the entire structure, which gradually shrinks and twists clockwise at approximately 120 degrees along the height of the building. According to the requirement of building function, the tower is divided into nine zones along its height by 8 sets of two-story outrigger system at each Mechanical/Electrical/Plumbing (MEP) floor [1]. Every zone has a specific usage function of either office, hotel, shopping mall or entertainment.

Like many other super tall buildings in the world, advanced design philosophies and innovative techniques



Fig. 1: Front view of three tallest buildings located in Lujiazui District, Shanghai

have been implemented into Shanghai Tower. For example, the double curtain wall system, the sustainable energy-saving concept, the mega column and core wall resisting system, as seen in Fig. 2 [2]. Considering its importance and complexity, many numerical analysis and even scaled laboratory shake table tests have been conducted on Shanghai Tower to investigate its structural performance, especially to predict its long-term behavior under extreme loading conditions that beyond the design standards [1, 3, 4].

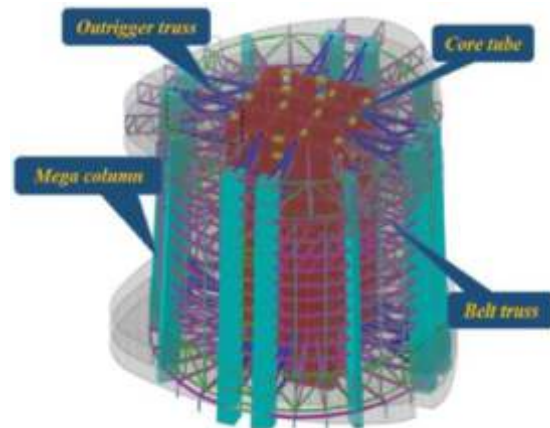


Fig. 2: Lateral resisting system of Shanghai Tower [2]

These models, even if well formulated based on highly idealized engineering drawings and best engineering judgements, may not accurately represent all mechanical and dynamic aspects of the structure, such as the material properties, boundary conditions and rigidity of nodes [5]. A significant discrepancy in terms of the dynamic characteristics between the actual building and the numerical model may exist due to large amount of uncertainties. Especially, for super tall buildings like the Shanghai Tower, more uncertainties and errors that are associated with the complex structural arrangements would be introduced into a more detailed FE model. Therefore, it is essential to conduct an output-only operational modal analysis (OMA) for this super tall building to identify its dynamic properties in real operation conditions with unknown excitation inputs (e.g., wind loads and live loads) [6], and then use the obtained information to tune and update a preliminary baseline FE model until the level of errors induced by the initial modeling is minimized. This procedure is normally called the FE model updating and the aforementioned OMA refers to an ambient vibration (AV) test.

In this paper, first presented is the full-scale ambient vibration (AV) test of the Shanghai Tower within the framework of a research project collaborated by the University of British Columbia (UBC) from Canada, Tongji University from China and the owner of Shanghai Tower. The field test was conducted at the final stage of construction of Shanghai Tower, aiming to identify the dynamic characteristics of this unique super tall building. This is followed by the development of an initial FE model of the Shanghai Tower based on the macro beam theory [7]. Next, a sensitivity-based automatic model updating is carried out by using the extracted modal properties from the AV test. Finally, results are discussed and the concluding remarks are presented.

## 2. OPERATIONAL MODAL ANALYSIS OF SHANGHAI TOWER

AV tests took place on May 8<sup>th</sup>, 2015 by a joint research team from UBC and Tongji University when the building was under final stage of construction. The whole test included two pre-setups (Setup X and Y) and four main setups (Setup A to D). The pre-setups (also refer to the collocation tests) were firstly conducted outside of the building to ensure that the internal clock of all the sensors were synchronized to a uniform time using GPS signals in the open air. Structural vibration sensor called TROMINO was used to carry out the AV test of Shanghai Tower [8]. Either GPS or Radio could be used to ensure synchronization between sensors. For this test, however, none of them were applicable since the signal was blocked by multiple building floors. Therefore, raw data collected by TROMINO was converted by Grilla software (provided by the developers of TROMINO) to a readable format first, and then the synchronization was performed manually via a MATLAB program and further refined in GEOPSY software based on internal clocks of the sensors [8-10].

In total, eleven floors (highlighted in red) were tested within four main setups, including all the strengthening MEP stories with outrigger truss, the ground floor and the lowest basement floor, as seen in Fig. 3. The owner of Shanghai Tower gave permission of only one day to perform the test, therefore additional floors or locations were not measured. All the sensors were placed at the opposite corner of core-tube in North-South (NS) direction in each floor due to accessibility restrictions. One TROMINO instrument (S1) was placed at a permeant location in the top floor (121F) as a reference sensor for the whole testing day and the rest six "roving sensors (S3-S8)" were moved in the sequential setups, as illustrated in Fig. 3.

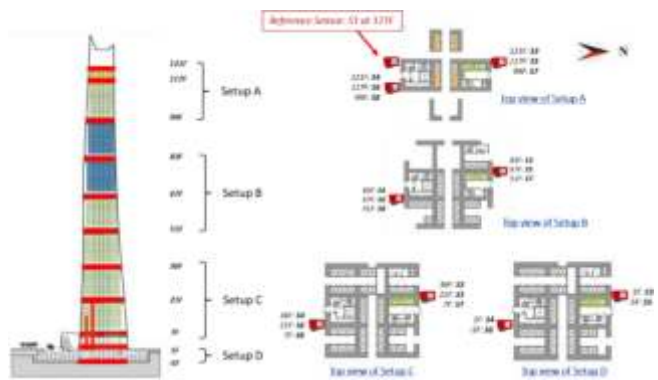


Fig. 3: Detailed arrangement of the AV test

Operational modal analysis was performed by using the software ARTeMIS Modal V3.6 [11]. For this project, FDD and EFDD were adopted and a simplified spatial representation of the lateral resisting systems of Shanghai Tower was established to visualize the corresponding mode shapes [6, 12]. FDD provides an efficient and quick manner for user to obtain the dynamic properties of the structure by peak-picking rules. As an extension of FDD, EFDD allows users to identify the damping properties of the corresponding modes.

In total, 9 modes below 1Hz and the corresponding damping values were estimated (period range from 0.1s to 10s), including 3 pairs of translational modes and 3 torsional modes, as shown in Fig. 4. It can be seen clearly that for this highly regular and slender super tall building, translational modes of each principal directions in each pair were closely spaced. The fundamental periods of the Shanghai Tower in

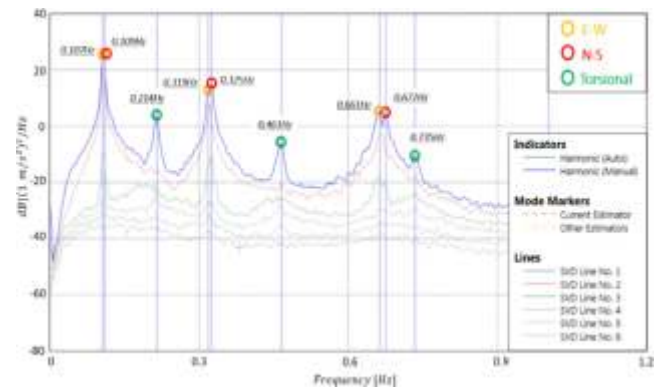


Fig. 4: Peak-picking of Singular Values of Spectral Densities

East-West (EW) and North-South (NS) directions are 9.38s and 9.18s with the corresponding damping ratios of 1.734% and 1.688%, respectively. The third mode is the first torsional mode with a period of 4.68s.

### 3. DEVELOPMENT OF THE BASELINE FE MODEL

The development of a baseline FE model is a starting point for updating. However, it is impractical to perform the iterative model updating for a detailed FE model of super tall building since extremely large number of elements and degree of freedoms would require huge computational workload. Therefore, in this study, a simplified lumped-mass stick model of Shanghai Tower was established in SAP2000 based on the macro beam theory that accounts for the effects of torsion, the story shear and bending deformations [7].

In this initial FE modeling, a story was represented by a macro beam member whose sectional properties, including the moments of inertia, location of centroid, shear area, were determined based on conventional beam theory. This method could reasonably simulate the horizontal and torsional vibration of super tall buildings with mixed wall-column components. The three-dimensional (3D) baseline FE model for Shanghai Tower is shown in Fig. 5. The model consists of 145 beam elements, 425 nodes with six degrees of freedom at each node. The translational and rotational mass at each level was assigned as a lumped mass at each story. A fixed-base assumption was made for simplification. The estimated Young's Modulus ranging from 36,000MPa to 41,740MPa were used from Zone 9 to Zone 1 of the building. A Poisson's ratio of 0.2 was adopted for the whole model.

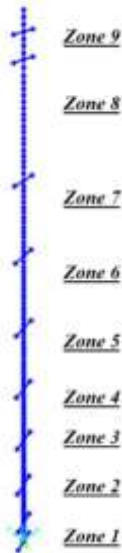


Fig. 5: Baseline FE model of Shanghai Tower

The calculated natural frequencies of first nine modes of the baseline FE model were listed in Table 1 for comparison. From Table 1, an average of 26% difference in frequencies was obtained between the measured data and the computed results from the FE model, especially the frequencies of torsional modes and higher translational modes.

Modes	OMA	Baseline FEM		MAC (%)
	Frequency [Hz]	Frequency [Hz]	Diff. (%)	
1	0.107	0.104	-2.43	77.7
2	0.109	0.104	-4.37	64.7
3	0.214	0.347	62.19	88.1
4	0.319	0.389	21.97	85.1
5	0.325	0.390	19.85	84.9
6	0.461	0.644	39.74	70.7
7	0.661	0.881	33.24	70.4
8	0.672	0.887	31.97	76.0
9	0.735	0.983	33.77	40.1

Table 1: Comparison of OMA and FEM results

### 4. FE MODEL UPDATING

A sensitivity-based FE model updating was conducted in this study with the aim to improve the analytical FE model for further dynamic analysis. The principle of this iterative method includes the calculation of the sensitivity matrices based on the selected target responses and structural parameters, and the formulation of the updated parameter vectors in each iteration [13]. The FE updating was performed by using the specialized FEMtools software where both the baseline FE model of Shanghai Tower and the obtained modal analysis results from AV test were imported into FEMtools [14]. The main updating procedure included three aspects: 1) correlation analysis, 2) sensitivity analysis for selection of updating parameters, 3) automated model tuning, as discussed in the following section.

To correlate the results between baseline FE model and OMA model, the modal assurance criterion (MAC) which is a correlation criterion in statistics was used in mode pairing. The correlation of dynamic properties for the first nine modes were presented in Table 1. All modes were well correlated with a minimum MAC of 0.7 except for the 2<sup>nd</sup> and 9<sup>th</sup> modes.

Selection of appropriate responses and updating parameters is the most important step to achieve a satisfactory model updating. However, it is difficult to decide which parameters of structural components in the FE model are preferred, and it is unrealistic to modify many physical parameters piece by piece. Therefore, in order to select proper variables and improve the updating efficiency, it is necessary to carry out the sensitivity analysis. Initially, all the possible uncertain parameters should be included, but parameters with low sensitivity should be eliminated before updating to achieve high efficiency [15]. Uncertainties in structural modeling are typically associated with material properties, section parameters and boundary conditions. For the baseline FE model of Shanghai Tower, the mass density ( $\rho$ ), Young's Modulus ( $E$ ) and cross-sectional area ( $A$ ) of all local macro beam elements were selected for sensitivity analysis. Torsional stiffness ( $J$ ) about vertical direction was also selected since large dispersion was observed in all three torsional modes. The uncertain bending moment of inertia ( $I_x$  and  $I_y$ ) about two translational directions were also taken into account for sensitivity analysis. In total, 90 most significant "global" parameters were studied with sensitivity analysis [14].

Fig. 6 shows the sensitivity matrix of bending moment of inertia in two principle directions. Physical meanings of selected parameters were well presented that both  $I_x$  and  $I_y$  have no effects on the torsional modes. It can be demonstrated that Shanghai Tower is a highly regular structure regardless of its outer rational façade since  $I_x$  and  $I_y$  only affect modes in its principle directions, namely EW and NS, respectively. In the meantime, all frequencies were not sensitive to changes of  $I_x$  and  $I_y$  in Zone 8 and Zone 9.

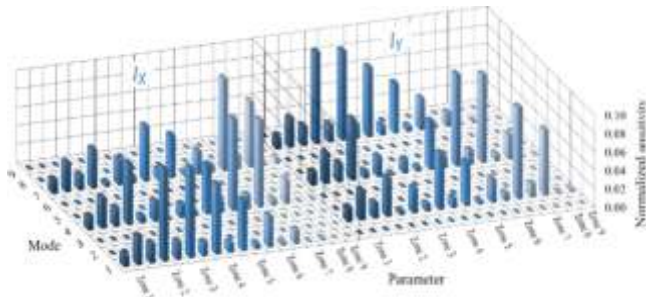


Fig. 6: Sensitivity matrix of bending moment of inertia

Table 2 summarized all the parameters for updating by removing all the insensitive ones. Physically realistic upper (+25%) and lower (-25%) limits for these parameters were estimated and also tabulated in Table 2.

Parameter	Allowed decrease (%)	Allowed increase (%)	Average change (%)
$\rho$	-30	30	+15.0
E	-25	25	-8.2
A	-30	30	+19.3
$I_x$	-25	25	-6.4
$I_y$	-25	25	-5.4
J	-30	30	-25.0

Table 2 Parameters selected for model updating

Automatic updating was carried out using the FEMtools program and converged within 10 iterations with minimum improvement 0.01% between two consecutive iterations. Fig. 7 presents a three-dimensional plot of MAC matrix after updating. Better MAC values were obtained and significant improvements were achieved for the 2<sup>nd</sup> torsional modes where the MAC increased from 70.7% to 81.9%. All the other modes also have a reasonable match with over 60% MAC values except for the 9th mode. This can be considered as an acceptable result considering the coupled torsional mode and local modes in the real structure, as well as the limited number of sensors for this super tall building. A summary of the final results is shown in Table 3. The average absolute difference of frequency is 4.4% after updating and the largest value 8.48% is below 10% error, indicating the success of the updating.

The parameter changes after updating could be found in Table 2. For the baseline FE model of Shanghai Tower, there is a decrease for all the stiffness related parameters. For instance, the torsional coefficient J was reduced by almost 25% in average from Zone 1 to Zone 9. More specifically, 17% decrease was found for Zone1, Zone 7-9, and 25% decrease was made for Zone 2-6. Smaller reductions in Young's Modulus E and moment of inertia for two directions

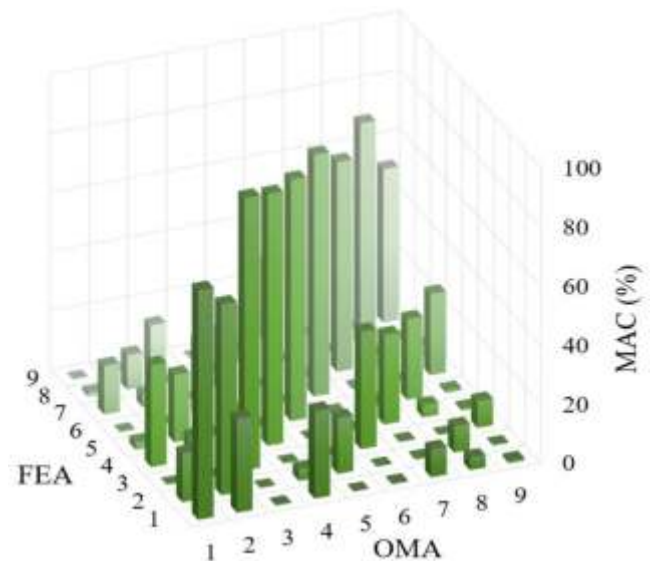


Fig. 7: MAC correlation after updating

were identified. On the other hand, since overall the periods of baseline FE model were smaller than the measurement results, mass related parameters were increased after updating, including the mass density  $\rho$  (+15%) and the cross section area A (+19%), respectively. Considering the lower and upper limits to the above mentioned parameters, the results are physically realistic.

Modes	OMA	Updated FEM		
	Frequency (Hz)	Frequency (Hz)	Diff. (%)	MAC
1	0.107	0.102	-3.96	77.8
2	0.109	0.103	-5.12	64.6
3	0.214	0.228	6.71	92.4
4	0.319	0.332	4.03	85.3
5	0.325	0.334	2.67	81.8
6	0.461	0.465	0.97	81.9
7	0.661	0.717	8.48	71.1
8	0.672	0.724	7.75	75.9
9	0.735	0.735	-0.02	52.0

Table 3 Results of automated FE model updating

In the end, the graphical comparison of all nine mode shapes of updated FE model and OMA model was shown in Fig. 8. From this figure, and the calculated MAC values and frequency differences, it is evident that the updated FE model is very close to the counterpart of the full-scale AV test of the Shanghai Tower.

## 5. CONCLUSIONS

This paper presented a comprehensive study of the ambient vibration test, finite element modeling and model updating of the tallest building in China, the Shanghai Tower. The full-scale field test was carried out by a joint research team from UBC and Tongji University, aiming to assess the dynamic characteristic of the structure at its final stage completion and provide useful information to calibrate the FE model for further dynamic analysis. Operational modal analysis was performed to identify the first ten modes and the corresponding damping ratios below 1Hz by using the



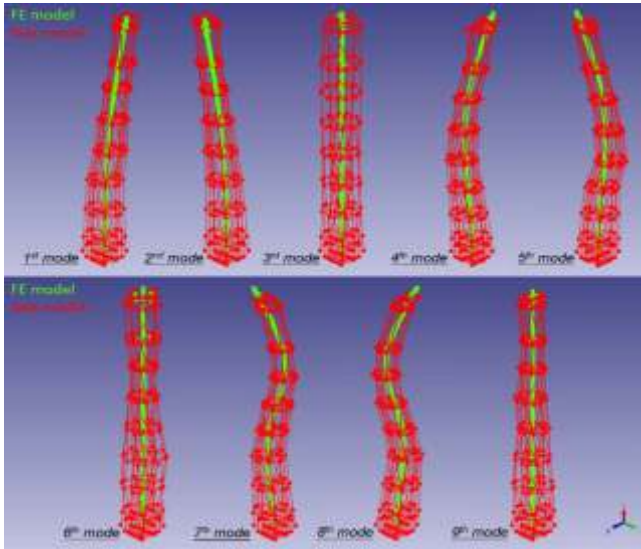


Fig. 8: Comparison of mode shapes between updated FE model and OMA model

FDD and EFDD techniques. As low as 0.107Hz fundamental mode was obtained in EW translational direction, and a closely spaced 2<sup>nd</sup> mode of 0.109Hz was identified in NS direction. A period of 4.7s was determined as the 1<sup>st</sup> torsional mode with a damping ratio of 0.86%. In general, Shanghai Tower behaved as a highly regular high-rise structure even though complex lateral force resisting systems and sophisticated architectural appearance were designed.

An initial FE model of Shanghai Tower that accounted for the torsional effect and shear deformation of mixed column/wall flexible high-rise structure was first developed on the basis of the design information. Six key parameters were then selected for updating based on the sensitivity analysis with physically reasonable upper/lower limits. Eventually, the automatic iterative model updating was successfully carried out. An average of 4.4% difference in frequencies of all nine modes was achieved between the updated FE model and the testing results. Good correlation of nine mode shapes and the corresponding MAC values were obtained both numerically and graphically. All parameter changes were within their physically acceptable limits and the updated FE model provided essential information for further nonlinear dynamic analysis and assessments under other loading conditions.

## ACKNOWLEDGEMENTS

The authors wish to thank the State Key Laboratory of Disaster Reduction in Civil Engineering from Tong University for their interest and support in this study. The assistance and permission to access to the building of the owner of Shanghai Tower is greatly appreciated. The authors would like to acknowledge the cooperation and enthusiasm from all the graduate students for assisting the AV test. Technical supports from Dr. Yavuz Kaya, Mr. Felix Yao, Mr. Xiang Li, and Mr. Yu Feng at EERF, UBC are well appreciated. The authors would also like to acknowledge Ms. Sharlie Huffman of the BC Ministry of Transportation for providing the instruments. A special thank is given to Dr. Palle Andersen of SVS for providing the license of ARTeMIS Modal.

## REFERENCES

- ♦ [1] Xiao Lu, Xinzhen Lu, Halil Sezen and Lieping Ye, "Development of a simplified model and seismic energy dissipation in a super-tall building," *Engineering Structures*, 67: p. 109-122, 2014.
- ♦ Jia-Zhan Su, Yong Xia, Lu Chen, Xin Zhao, Qi-Lin Zhang, You-Lin Xu, Jie-Min Ding, Hai-Bei Xiong, Ru-Jin Ma and Xi-Lin Lv, "Long-term structural performance monitoring system for the Shanghai Tower," *Journal of civil structural health monitoring*, 3(1): p. 49-61, 2013.
- ♦ [3] Huanjun Jiang, Liusheng He, Xilin Lu, Jiemin Ding and Xin Zhao, "Analysis of seismic performance and shaking table tests of the Shanghai Tower," *Jianzhu Jiegou Xuebao (Journal of Building Structures)*, 32(11): p. 55-63, 2011.
- ♦ [4] Dennis CK Poon, Ling-En Hsiao, Yi Zhu, Leonard Joseph, Steve Zuo, Guoyong Fu and Onur Ihtiyar, "Non-linear time history analysis for the performance based design of Shanghai Tower," *Structures Congress 2011*. 541-551, 2011.
- ♦ [5] Dora Foti, Vincenzo Gattulli and Francesco Potenza, "Output-Only Identification and Model Updating by Dynamic Testing in Unfavorable Conditions of a Seismically Damaged Building," *Computer-Aided Civil and Infrastructure Engineering*, 29(9): p. 659-675, 2014.
- ♦ [6] Rune Brincker, Lingmi Zhang and Palle Andersen, "Modal identification of output-only systems using frequency domain decomposition," *Smart materials and structures*, 10(3): p. 441, 2001.
- ♦ [7] Y Liu, R Chen, Y Jiang and W Liu, "Lumped-Mass Stick Modeling of Building Structures with Mixed Wall-Column Components," *Proceedings of 15th World Conference on Earthquake Engineering (15WCEE)*. 2012, Lisbon, Portugal.
- ♦ [8] Micromed, "Tromino User's Manual," *Micromed*: p. 139 pp, 2012.
- ♦ [9] MathWorks, "Matlab: High performance numeric computation and visualization software, User's Guide," 2015, Natick, MA
- ♦ [10] M Wathelet, "GEOPSY Geophysical Signal Database for Noise Array Processing, Version 2.9.0 2002-2011.," 2005, Grenoble, France
- ♦ [11] SVS, "Artemis Extractor Pro 1999-2015. Version 3.6, NOVI Science Park, Structural Vibration Solutions A/S," 2015, Demark
- ♦ [12] Niels-Jørgen Jacobsen, Palle Andersen and Rune Brincker, "Using enhanced frequency domain decomposition as a robust technique to harmonic excitation in operational modal analysis," *Proceedings of ISMA2006: international conference on noise & vibration engineering*. 18-20, 2006.
- ♦ [13] Stana Živanović, Aleksandar Pavic and Paul Reynolds, "Finite element modelling and updating of a lively footbridge: The complete process," *Journal of Sound and Vibration*, 301(1): p. 126-145, 2007.
- ♦ [14] DDS, "FEMtools user's guide, version 3.8.2, Dynamic Design Solutions NV (DDS).", 2016, Leuven, Belgium.
- ♦ [15] KATL Kodikara, THT Chan, T Nguyen and DP Thambiratnam, "Model updating of real structures with ambient vibration data," *Journal of Civil Structural Health Monitoring*, 6(3): p. 329-341, 2016.

# Analysis of the concept: Seismic Resilience

Juan Carlos Flores<sup>1</sup>, Mabel Mendoza<sup>2</sup>, Hugo Castellanos<sup>3</sup>

<sup>1</sup> Faculty of Engineering, UNAM, Mexico

<sup>2</sup> Department of Structures, Faculty of Engineering, UNAM, Mexico

<sup>3</sup> Grupo CCEIC, Mexico

**Abstract:** Seismic resilience can be achieved by reducing the probabilities of failure of a system during an earthquake, as well as reducing the consequences of such failures and their recovery time. This paper explores the resilience concept doing a first approach from the psychology field and then from the mechanics of materials. The characteristics and elements of seismic resilience are defined and the mathematical functions that describe the behavior of the phenomena of resilience are analyzed, a special emphasis is done on recovery time as key element of resilience and its quantification, finally some proposal designs based on resilience are presented.

## 1. INTRODUCTION

Throughout history society has always faced major disasters of natural and anthropic origin. With the evolution of society and the development of new communities with increasingly complex organizational, political-economic and infrastructure systems, to be prepared and be able to recover in an optimal way in short periods from contingencies and sudden changes in the conditions of communities, has become a great necessity.

In the World Conference on Disaster Reduction held in Kobe, Japan in 2005, the importance of including the concept of resilience in the response context to natural disasters was confirmed. However, resilience is a broad term that is used in many disciplines with similar definitions, adapted to each research field.

The Rockefeller Foundation started in 2013 the 100 Resilient Cities program *100RC*, which objective is to encourage the adoption of *urban resilience programs* in the great capitals of the world, so they can be able to respond in a more adequate way to natural disasters and social problems.

Mexico City was one of the first members of the 100RC and in November of 2015 hosted the Second Global Resilience Directors Summit, with the objective of sharing experiences, strategies and activities that have been carried out in other cities of the network to achieve resilience.

In Mexico as nation, due to its geographical location it is of special interest for civil engineering the analysis of the concept of resilience from a seismic approach since these kind of natural events have had the greatest impact along the country.

## 2. RESILIENCE IN SOCIAL CONTEXT

Blascovich (1996) indicates that since the 90s, a

considerable number of publications that seek to describe characteristics and conditions of resilient individuals in diverse social, economic and health situations have been made.

Luthar and Cicchetti (2007) define resilience as a dynamic process where individuals show a positive adaptation despite experiences of significant adversity or trauma, they also point out that the term does not represent a feature or attribute of the subject's personality rather is a two-dimension construction that implies the exposure to adversity and the manifestation of positive results.

Other authors such as Manciaux et al. (2003) do not restrict the concept only to individuals and define it as the capacity of a person or group of people to develop correctly to continue projecting themselves into the future despite the destabilizing events, hard life conditions and severe traumas.

Three phenomena are distinguished in social resilience:

- People under a risk situation show results that succeed the expectative;
- Positive adaptation continues despite the presence of stressing experiences and;
- There is a good recovery from traumas.

The relation between social resilience and the mechanics of materials was first established by Bowly (1192) who used the concept, strength of a material, figuratively and defined it as a *moral spring or elastic, a person who does not*

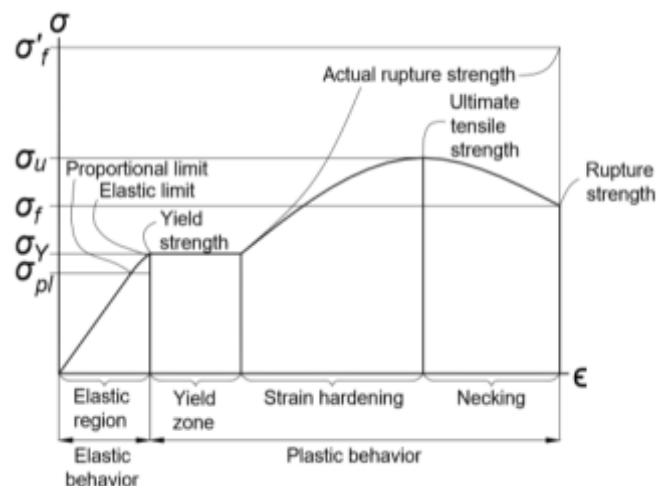


Fig. 1: Stress-strain diagram of a ductile material

discourage, that does not give up.

### 3. RESILIENCE OF A MATERIAL

The strength of a material depends on its capacity to withstand a load without excessive deformation or failure. This property is inherent in the material itself and must be determined by experimentation (Hibbeler, 2011).

Compression and stress tests in materials are the most common, the results are translated into stress-strain diagrams, where the ordinate axis corresponds to the stress, obtained from dividing the applied load ( $P$ ) by the area ( $A$ ) of the initial cross-section of the material.

$$\sigma = \frac{P}{A} \quad (1)$$

The abscissa axis correspond to the strain ( $\epsilon$ ) and which is result of dividing the length change ( $\delta$ ) by the initial length of the sample ( $L$ ).

$$\epsilon = \frac{\delta}{L} \quad (2)$$

It should be noted that the obtained diagrams from identical samples of the same material will never be identical due to several factors that influence the tests. In figure 1 it is showed the typical stress-strain diagram, of a ductile material.

Figure 2 highlights the elastic region of a stress-strain diagram which is limited by the proportional limit. In this region materials have the capacity to recover their original dimensions once the applied loads are removed. A linear relation is presented between stress and strain, this phenomenon is known as Hooke's law and mathematically is defined as:

$$\sigma = E\epsilon \quad (3)$$

The variable ( $E$ ) depends on each material and represents a proportionality constant called modulus of elasticity or Young's modulus.

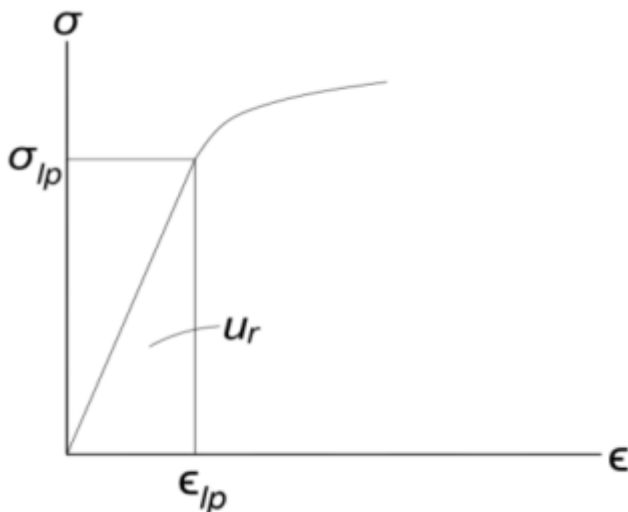


Fig. 2: Elastic region of the diagram

It is identified as deformation energy to that which is stored by the material due to the deformation caused by external loads. It is in the elastic region where the materials resilience appears and it physically represents the ability of the material to absorb energy without permanent damage on it (Hibbeler, 2011).

The resilience modulus ( $u_r$ ) of a material can be expressed by the next equation:

$$u_r = \frac{1}{2} \sigma_{Ip} \epsilon_{Ip} = \frac{1}{2} \frac{\sigma_{Ip}^2}{E} \quad (4)$$

Where  $\sigma_{Ip}$  and  $\epsilon_{Ip}$  are the stress and strain under the proportional limit and  $E$  is the modulus of elasticity.

Riley (2001) defines the resilience modulus as the maximum deformation energy per volume unit that a material will absorb without inelastic deformation.

In the field of pavement design, the cyclic nature of the loads acting on the different layers of the pavements generates elastic or resilient deformations, where the materials recover their original thickness, and plastic deformations. Resilient deformations are of instantaneous recovery while plastic ones remain when the loads have ceased. Under the action of mobile loads the deformation accumulates but decreases with each cycle until it is almost null in the final ones, the sample can reach a point where all the deformation is recoverable and is said that the material has adopted a resilient behavior. The resilience modulus is defined as the repeated deflection stress applied in triaxial compression divided into the recoverable axial deformation.

### 4. SEISMIC RESILIENCE

In the seismic engineering field, resilience can be achieved by reducing the probabilities of failure of a system during an earthquake, as well as reducing the consequences of such failures and their recovery time.

Bruneau (2003) points out that, a resilient system is only the one that shows the following characteristics:

- Reduced failure probabilities.
- Decreasing of the failure consequences in terms of loss of lives, damage and negative economic and social consequences.
- Short recovery time, recovery of a specific system or systems group to their normal operation level.

Resilience can be expressed as a function that indicates the ability of a system to sustain certain level of functionality or performance during a determined period.

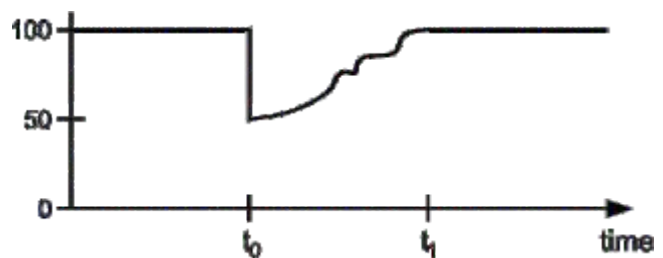


Fig. 3: Schematic representation of resilience as a function of time

Figure 3 shows the function in the range from 0% to 100%, where 100% represents an absence of damage and 0% a total loss of functionality of the system. The occurrence of an earthquake with such magnitude that could reduce the system's quality by 50% is assumed. It is expected that restoration occurs from  $t_0$  to  $t_1$ , when functionality has been completely recovered. Therefore resilience loss ( $R$ ) can be determined by the magnitude of the degradation over time, mathematically defined by:

$$R = \int_{t_0}^{t_1} [100 - Q(t)] dt \quad (5)$$

Recovery time is a variable with a high level of uncertainty due to the factors that influence it, it usually depends on the earthquake's intensity, but constructive methods and the assignation of resources also modifies its behavior.

Cimellaro (2010) proposes different functions (linear, trigonometric, and exponential) that can approximately represent recovery time and describe how well prepared is a system to any contingency.

Lineal function is the simplest and is usually used when there is not enough information about resources assignation to the system's recovery or about the response of society (Fig. 4).

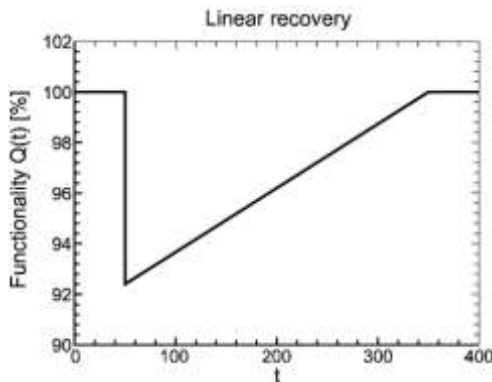


Fig. 4: Function of time of linear recovery

If social response and recovery process are imitated by the amount of resources or lack of organization, a trigonometric function is used (Fig. 5).

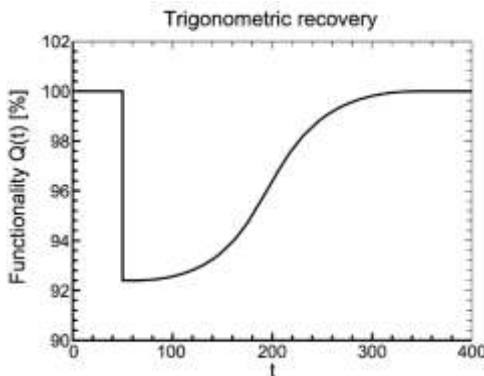


Fig. 5: Function of time of trigonometric recovery

Exponential functions can represent a recovery process with an initial generous resources flow where its speed decreases as the process ends.

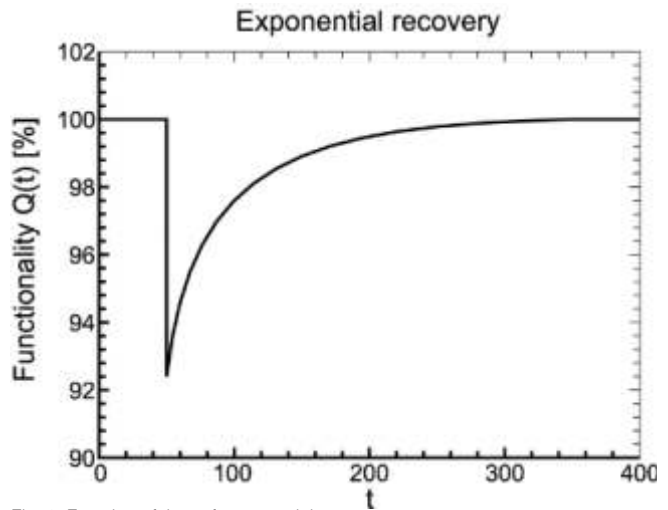


Fig. 6: Function of time of exponential recovery

Bruneau and Reinhorn (2006) establish that resilience of physic and social systems consists of 4 properties or dimensions.

- Robustness: strength, or the ability of the elements, systems and other analysis measures to withstand a determined level of stress or demand without degradation or functionality loss.
- Redundancy: the extent to which elements within a system exist that can be replaced in case of disruption, degradation or loss, without it fail to function properly.
- Resourcefulness: the ability to identify problems, prioritize and mobilize resources when existing conditions threaten to disrupt any element function, it can also be conceptualized as the ability to assign resources (monetary, physical, technological, computer or human) to the recovery process in order to achieve established goals.
- Rapidity: the capacity to recover optimal functionality in the shortest possible time.

Figure 7 shows a representation of figure 3 with an addi-

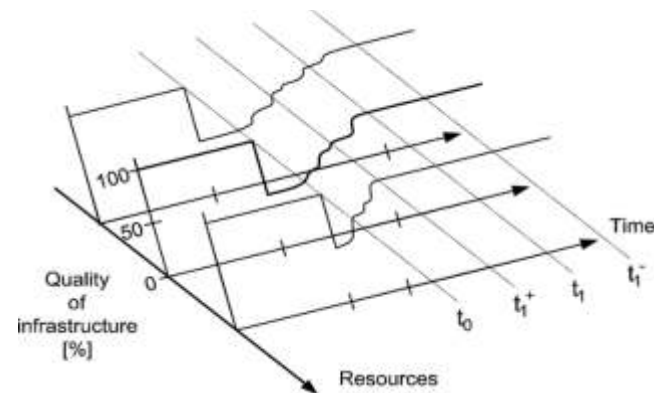


Fig. 7: Tridimensional resilience representation

tional dimension which represents the resources assignment and its impact in the recovery time of the system.

Redundancy can be represented as a system formed by a group of several elements with similar functions inside a specific geographic area (Fig. 9), though, links between these elements may be systems with distinct nature, such as the case of a healthcare network where hospitals are connected by the roads and highways community network, hence seismic resilience of the healthcare network largely depends on that of the roads and highways system.

Seismic resilience can be divided into resilience of structural elements and of non-structural elements, for practical purposes both can be grouped under the integrity concept. Figure 8 presents different integrity loss levels, each one portrays an affectation level of the distinct elements.

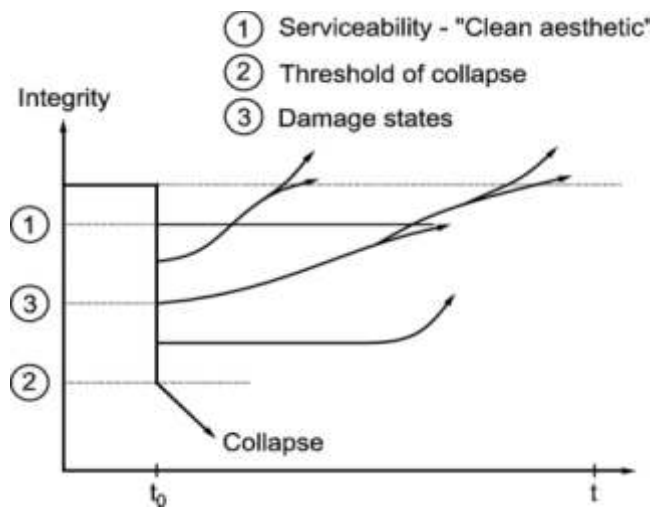


Fig. 8: Resilience defined by integrity

Level 1 shows a small integrity loss where damage to the aesthetic of the building but not to the structure can be assumed, level 2 indicates the collapse of the structure, between both levels can exist many damage states (3).

It is also shown that over time restoration can reach lower or higher levels of seismic performance than the initial the initial one depending on the type of repairs or improvements added.

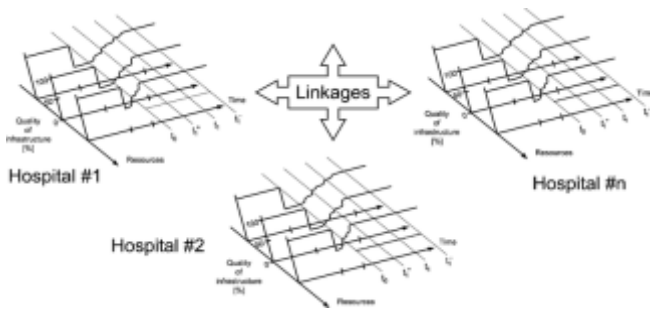


Fig. 9: Resilience as a concept of 4 dimensions applied to a healthcare network

### 5. QUANTIFICATION OF SEISMIC RESILIENCE

Bruneau and Reinhorn (2007) establish as resilience quantification method the use of tridimensional bell-curves

that in 2D form can be seen as isoprobability curves, inside an orthogonal space delimited by soil pseudo-accelerations and the inter-story drifts of the structure, this concept is known as Sliding an Overlaid Multidimensional Bell-curve of Response for Engineering Resilience Operationalization in an Orthogonal Limit-space Environment, SOMBRO in OLE, inside OLE service and failure limit states are set, therefore, the probability of the structure to exceed a limit state can be calculated as the volume of the area under the curve which surpasses the line of a specific limit (Fig. 10).

There are two response cases, there first one is a linear-elastic response that can be translated as no significant intersections between isoprobability curves and limit states that can represent damage to nonstructural elements. It is expected that the magnitude of intersections increases with the earthquake return period.

In the second case exists a nonlinear-inelastic response, it differs from the first one because in this one exists structural damage, with the SOMBRERO in OLE concept resilience can be quantified since there exist significant intersections, as the last case it is expected that the magnitude of the intersections increases with the earthquake return period. It must be considered that the occurrence of consecutive earthquakes affects considerably the probability of exceeding limit states.

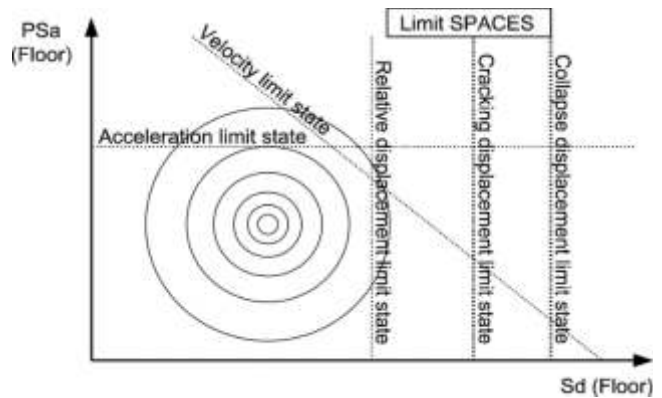


Fig. 10: SOMBRERO in OLE and limit states

Fragility curves, function of the threat that an earthquake represents, are used to express the probability to reach a limit state. Figure 11 shows the probability of exceedance in 50 years before  $t_{e-}$  and after  $t_{e+}$  an earthquake.

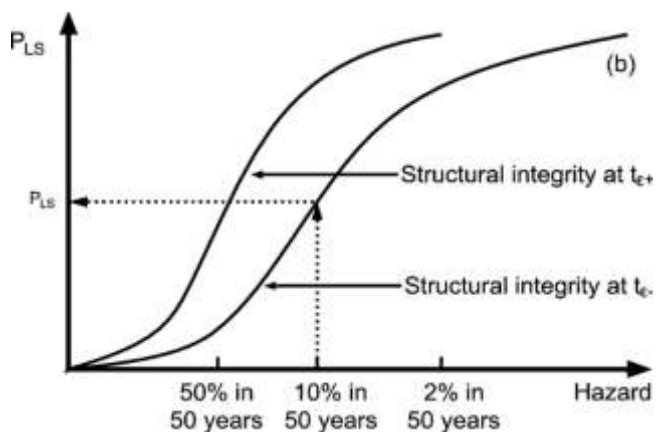


Fig. 11: Fragility curves of a structure

Resilience quantification is a valuable resource that must be handled with care and interpreted correctly. The value obtained from the resilience loss with equation 5 can be interpreted as an area under a curve, figure 12 displays two areas with identical magnitude, however, both have a completely distinct impact on the structure performance, the first one shows a total loss of functionality during a short period (a), the second presents a small reduction but for a long time (b), this does not mean that the calculated value is incorrect but it identifies resilience as a "non-linear concept".

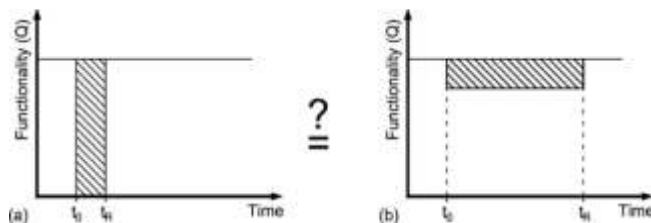


Fig. 12: Resilience non-linearity

For each system functionality loss is differently perceived, in the case of service providers, they prefer a scenario in which the number of affected users is the minimal. On the other hand, users prefer a case where all lose the service for a short period than be part of the unlucky relatively small group that loses the service for a longer one. Recovery cost is again an important factor since for some systems recover functionality from zero has a higher economic impact than recover it slowly from a minor damage that is the case of a healthcare network.

## 6. DESIGNS BASED ON SEISMIC RESILIENCE

According to An and He (2016) there are two methods to improve the resilience of structures, the optimization of the structural system, which includes the design of the components and its set up, and the implementation of isolation and energy dissipation devices.

The first option is useful when the structure has "weak layers", since modifications can be done without significant alterations to the system's functionality and with a good cost control, however, when the structural system is simple and there are only few elements, optimization is limited.

Isolation and energy dissipation devices are additional components that absorb seismic energy and reduce vibration and deformation of the main structure, as an advantage, they can be replaced in short time after failure. When a structural system cannot be optimized this is an efficient way to improve seismic resilience.

Hogg (2015) mentions that since 2011 a considerable number of buildings that illustrate the different available resilience technology have been constructed in New Zealand. The implemented elements in many structures include:

- ♦ Concave friction slider base isolation.
- ♦ Pre-stressed ring-feder hold down springs.
- ♦ Compression and tension yielding energy dissipaters.
- ♦ Compression and tension yielding buckling restrained braces.

- ♦ Replaceable frame shear links
- ♦ Sliding friction joints.

After Canterbury earthquake in New Zealand in 2011 communities as Christchurch and Nelson were severely affected. As part of restoration works of the Knox Church in Christchurch, a system of plug and play energy dissipaters was implemented at the base of the rocking buttresses (Fig. 13) in such way they could be easily replaced if they were damaged.



Fig. 13: Plug and play energy dissipater on the base of a buttress

Other devices like lead rubber base isolation bearing are more common in many buildings around the world due to their good performance and low cost (Fig. 14).



Fig. 14: Lead rubber base isolation bearings in the second floor of the Mexico-Puebla highway

## 7. CONCLUSION

Initially as a characteristic of the materials, the concept of resilience has adapted to many disciplines, nevertheless, in all of them it describes positive phenomena to adversity situations.

Seismic resilience is a concept that seeks an adequate response of buildings, through specific characteristics such as robustness, redundancy, resourcefulness and rapidity, to earthquakes; minimizing damages and their consequences as well as the recovery time of these, which plays a significant role in the quantification of resilience and that is widely affected by conditions of the community where the

building is located.

Despite being a useful concept, the result of resilience quantification must be interpreted properly due to its non-linear nature and the different way it affects the systems.

With the technological development, structural design based on seismic resilience has become possible, resorting mainly to the optimization of structural elements and its set up or to isolators and energy dissipaters, these designs can be adapted to existing infrastructure to improve its seismic behavior.

## REFERENCES

- [1] Oficina de Resiliencia CDMX, *Estrategia de resiliencia CDMX*, 2016, Mexico.
- [2] Sara Alejo Vázquez, *Comparación de algunas definiciones de resiliencia en la psicología social*, 2012, Mexico.
- [3] Russell C. Hibbeler, *Mecánica de Materiales*, 8<sup>th</sup> edition, 2011, Mexico.
- [4] William F. Riley, Leroy D. Sturges and Don H. Morris, *Mecánica de Materiales*, 2001, Mexico.
- [5] Paul Garnica A., Natalia Pérez G. and José A. Gómez L, *Módulos de resiliencia en suelos finos y materiales granulares*, 2001, Mexico.
- [6] Michel Bruenau and Andrei Reinhorn, *Overview of the Resilience Concept*, 2006, USA.
- [7] Michel Bruenau and Andrei Reinhorn, *Exploring the Concept of Seismic Resilience for Acute Care Facilities*, 2007, USA.
- [8] Gian Paolo Cimellaro, Michel Bruenau and Andrei Reinhorn, *Framework for analytical quantification of disaster resilience*, 2010, USA.
- [9] Ning An and Zheng He, *A Framework of Seismic Design Based on Structural Resilience*, 2016, Canada.
- [10] S. J. Hogg, *Seismically Resilient Building Technology: Examples of resilient buildings constructed in New Zealand since 2013*, 2015, Australia.

# Ancient building material is re-engineered

**B**uildings made of cob have survived through the years as it is a very durable material. Researchers are now trying to produce a material based on cob with increased thermal insulation. The project is led by Steve Goodhew, professor at the University of Plymouth.

The new material is called CobBauge (a name that combines English and French words).

The first part of the project which will finish in the end of March, 2019, includes research on how to increase cob's ability to trap heat inside structures. To achieve this, researchers have used 2 grades of cob: A lightweight version with good insulating properties and a stronger version to increase the material's total strength.

"What we're doing is taking a robust vernacular material and bringing it right up-to-date. While what we have come up with is without a doubt a modern interpretation of cob, we hope it will satisfy both the traditionalists, and those looking for a hi-tech, energy-efficient material. As a result of this research, we can say there is no reason why cob cannot be used to build modern houses that meet the latest standards," Goodhew said.

According to the European Union, CobBauge can significantly reduce the demand for heating and cooling of buildings, a fact that is important to meet the climate



goals Europe wishes to achieve. Moreover, the production and usage of cob will greatly reduce CO<sub>2</sub> emissions and construction waste in comparison with traditional masonry materials.

The team's next target is to build one or more structures with this material to test its performance in real scale. "Here we'll be studying real CobBauge buildings, subject to real environmental conditions over a prolonged period to investigate in-situ thermal performance, humidity, particulates, the presence of volatile organic compounds (VOCs) and related energy use," researcher Jim Carfrae, stated.

# Spline arch – A pneumatic Chamber system applied in a temporary membrane structure

Juan Jose Ramirez<sup>1\*</sup>  
1\* CEO, HYPARCH, México

**Abstract:** This work is about the feasibility of using slender elements combined with pneumatic chambers as support structural elements in temporary membrane structures applications.

Spline term in this work refers to those straight and slender elements that are bent to form a continuous spatial curve and identical moment of inertia (second moment of area) about any axis perpendicular to its centroidal axis. It is common to use arches as supporting elements in membrane lightweight structures. There are very few applications of spline elements combined with membranes in medium – large span structures. Applications in small spans are more common for example in camping tent systems where spline elements are stiff enough to take external forces. For medium (16 – 32 m) span structures it is common that spline elements need in-plane bracing systems formed by masts and cables, in order to increase stiffness and strength properties to be able to bare real external forces (wind or snow). It is included the use of pneumatic chambers instead of mast-cables system in order to make spline arches stiff enough to withstand real external forces.

## 1. INTRODUCTION

It is very important to design and develop structural systems as simple and lightweight as possible in order to be environmentally friendly. This work is intended to be another step in the structural engineering field in terms of lightweight structures development. There are actually some structural applications involving spline elements combined with compression and tension (mast-cables) elements used in lightweight membrane structures in order to develop stiff enough and force resisting systems to solve supporting frame components. There's theoretical and experimental knowledge about pneumatic chambers or cushions used in structural engineering and it is the idea of this work to use it in order to develop this hybrid spline-pneumatic chambers structural element.

The aim of this work is to evaluate the feasibility of the use of pneumatic chambers as a real alternative being implemented in spline elements in order to make them stiff enough to withstand buckling and to resist forces arising from pre-bending erection stresses and from real loading conditions.

The hypothesis of this work is that "Implementation of pneumatic chambers in specific zones of a spline element generates stable arch support system for medium-span

temporary deployable membrane structure".

An analytical case study is developed. The solution of the structural system and demonstration of the stability, applied to 16 m span membrane structure supported by spline arch, are expected results. It is also included a proposal of the erection process.

## 2. SPLINE STRUCTURAL SYSTEMS (FROM DESIGN TO ERECTION PROCESS)

The term "spline structure" is adopted in this work, Adriaenssens (2000), to describe those structural elements that initially are straight and then bend into a spatial continuous curve having an identical moment of inertia (second moment of area) about any perpendicular axis to its centroidal axis. Such an element gets special importance when it is considered in the main structural supporting system of membrane structures because of some advantages listed below:

- ♦ Lightweight.
- ♦ Usable as a part of the erection process and then keep it as structural supporting system element once the structure is operating normally.
- ♦ The ability to take a different shape depending on the construction stage because of its flexibility.
- ♦ Combined with bracing systems, it can provide enough stiffness to the system in order to be capable to bare external loads like wind or snow.
- ♦ It can be extremely slender because it is continuously restrained from buckling by the membrane.

Some special properties need to be fulfilled by spline elements. Firstly, it needs to be flexible enough in order to be curved and keep deformations into the elastic range, this flexibility deals with material and geometry properties of the section. Once it is bent into the final shape, it has to resist forces arising from loading conditions (wind or snow), and finally it has to be stiff enough to withstand buckling. In this thesis the main aim is to propose a hybrid system composed by spline element plus pneumatic chambers inplane bracing system providing additional bending stiffness and demonstrating the feasibility of its use in real medium span projects.

ASTM A-36 Steel, aluminum, bamboo, GFRP and CFRP were evaluated, see table 1. Adequate materials for bending-active structures offer a ratio of  $\sigma/E \leq 2.5$ . Steel is not adequate for bending active structures.



When some members or the entire structure reach yield, ultimate strength, fracture, collapse or exceed specific maximum deflection, it is considered that structures can fail. Buckling refers to an event where a structural element subjected to compression forces deviates from a behavior of elastic shortening within the original geometry undergoing large deformations involving a change in shape for a very small increase in load. There are many other forms of instability that are generally also referred to as buckling. Lateral – torsional buckling is out of plane buckling phenomenon, but it is considered in this thesis that pre-stressed membrane gives lateral bracing to be stiff enough to avoid it.

An open source script written in grasshopper for rhino as a tool to obtain the shape of "the elastica" is used in this thesis. The script is based on the work of M. E. Pacheco "The elastic rod", where the differential equation is solved exactly in terms of Jacobi's elliptic functions finding the solution with an iterative method, varying some parameters of the elliptic functions.

In this work, the concept of pneumatic structure is adopted to those flexible membranes that derive their stability from air pressure.

There is a large variety of materials which can be used in pneumatic structures that depend mainly on the size of the project. For small structures, natural (cotton) or synthetic membranes are used. For large scale projects, stronger membranes materials are used, such as glass fiber, nylon or polyester, protected by a Teflon or vinyl layer. In large, permanent structures, such as stadiums, the best choice is regularly glass fiber with Teflon, although it is inflammable, it presents less deformability.

The larger the structure gets, the larger the tension to which it is submitted, which forces us to add a cable system to transfer tension and force to specific points. There are also two general types of pneumatic structures, depending on how they are inflated.

Air supported (low pressure systems)

Air inflated (high pressure systems)

The design process of tension structures, including air support systems, can be divided into three subprocesses, form finding, structural analysis and cutting pattern generation. The result of form finding subprocess is a shape of equilibrium for a certain stress distribution and boundary conditions. Then from this geometry, structural analysis is developed and cutting pattern is made. It is common in practice to separate and not interact these three subprocesses and it leads in built structures to highly inhomogeneous stress distributions that can be seen in wrinkles and measured in stresses that are bigger than required. An enhanced design concept is based on 5 steps: defining the shape of equilibrium (form finding), generating the cutting patterns, reassembling and pre-tensioning the cutting patterns, structural analysis of reassembled structure and evaluation of structural behavior.

Structural analysis process deals with material properties, forces considerations, and geometrical modeling assumptions. The hybrid system implies a

pneumatic part, spline arch, and cables. Specially designed software (EASY) is used to develop form and statical analysis for pneumatic chambers coupled with spline arch in this chapter. Dlubal RSTAB software is also used to make section assignments and results interpretation easier.

The form-finding process was carried out with EASY software using force density method. In the volume form-finding module, it is considered that the net is generated by force densities either inner pressure or volume. The main attributes in EASY that control pneumatic structures are: volume (V), pressure (P) and temperature (T). Relations of those attributes are governed by Boyle-Mariotte law.

In chapter 2, it was decided to use Glass Fiber Reinforced Plastics (CFRP) pipe for the spline arch element because its properties fit very well on spline structure needs in terms of modulus of elasticity ( $E = 165 \text{ GPa}$ ), allowable stresses ( $\sigma_M = 2800 \text{ MPa}$ ), low weight (Vol. Weight =  $24.9 \text{ kN/m}^3$ ) and resistance to corrosion. Section diameter of the pipe is  $90 \text{ mm}$  and wall thickness =  $5 \text{ mm}$ .

For the cable element, it is considered to use galvanized steel with a modulus of elasticity  $E = 160 \text{ GPa}$ , and Vol. Weight =  $80 \text{ kN/m}^3$ .  $13 \text{ mm}$  diameter cable was considered.

In the case of the membrane that will be used for pneumatic chambers, PVC coated polyester fabric (Ferrari Preconstraint 502) is considered. It is common that warp direction is a little bit stiffer than weft direction with different modulus of elasticity  $E_{\text{warp}} = 0.8 \text{ MN/m}$ ,  $E_{\text{weft}} = 0.6 \text{ MN/m}$ , assuming cross stiffness  $E_c = 0.3 \text{ MN/m}$  and shear modulus  $E_s = 0.03 \text{ MN/m}$ . In terms of weight,  $550 \text{ g/m}^2$  and  $0.6 \text{ mm}$  thickness was used.

Once properties and sections are assigned to the model there are considered realistic loading conditions in this work. In LOAD CASE 1, self-weight + pre-stress ( $1 \text{ kN/m}$ ) is considered. For wind loading it is supposed a basic pressure  $p = 0.5 \text{ kN/m}^2$  acting in three different attack angles  $0$  degrees,  $45$  degrees and  $90$  degrees, so LOAD CASE 2: self-weight + pre-stress + Wind  $_{0\text{degrees}}$ , LOAD CASE 3: self-weight + pre-stress + Wind  $_{45\text{degrees}}$  and LOAD CASE 4: self-weight + pre-stress + Wind  $_{90\text{degrees}}$ .

Because it is not possible to model tension membrane structure + pneumatic spline arch in EASY software it was necessary firstly to model supported membrane without spline arch, then calculate reactions under load cases described before and finally load spline arch model with those previously calculated reactions.

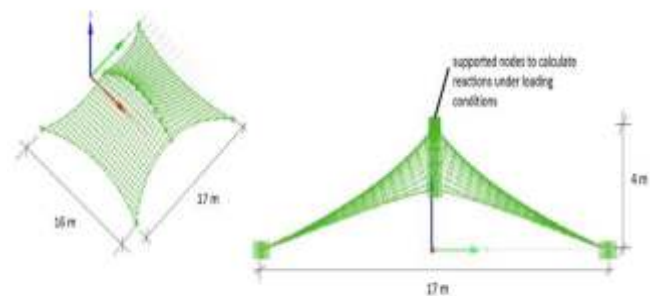


Figure 1: Membrane model (front elevation and perspective view), to evaluate loads in arch (Beam module, EASY software)

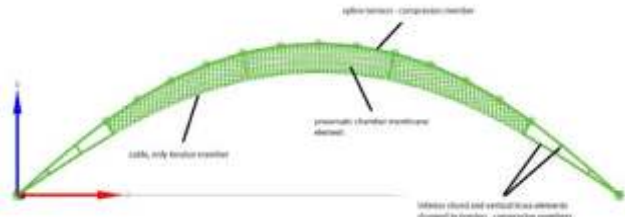


Figure 2: Final geometry components hybrid system (Beam editor, EASY software).

Most of the times special analysis considerations in models have to be reflected in structural detailing process. There are so many ways to connect structural elements in models and results from one way or another can be substantially different, for example if in the model it is supposed that the arch is moment released in one direction and not released in another one, in the support nodes, it is needed to take into consideration physically in fabrication process and connections details must be defined. It is intended to propose basic drawings and connection details of the most important parts of the system.

Erection process is one of the main reasons of the development of this work because it was inspired in the advantage that spline structures represent to the fast installation process. Transportation of materials is considered to be easy and short space required, it is considered the maximum length of CFRP pipes = 2.04 m, then system is composed of 7 pipes of 2.04 m length and 2 pipes of 1.49 m. The first step is to put all pipes in the ground and attach them together.

Once 9 pieces of pipes are joined together (see section 4.3 for connections and details), the next step is to put special connections at the beginning and ending pipes to connect a cable and induce axial forces and produce buckling on spline element (total length = 17.26 m). When spline element is buckled enough, supports must be fixed in the ground and a security cable must be attached to avoid uncompressing of spline element. The next step is to connect special aluminum profiles proposed to attach pneumatic chambers and fabric layer. Now it is the moment to attach non-inflated pneumatic chambers on the correct position to start inflation process. When pneumatic chambers are inflated then inferior chord cable and vertical truss elements must be connected to provide the system enough stiffness to be able to attach membrane and start erection process.



Figure 3: Hybrid system ready to attach membrane (erection process)

### 3. CONCLUSION

Real wind loading conditions have been considered during the development of this work in terms of a constant pressure of  $0.5 \text{ kN/m}^2$ . This value is a good approach of an average value in Mexico talking about temporary structures. It is demonstrated the feasibility of the use of the pneumatic system to increase the stiffness of the spline element from an analytical point of view considering a convergence criteria to evaluate the stability of all the structure.

Because of software tools (used in this work) limitations, it was not possible to model both membrane cover and hybrid pneumatic system together, and it was necessary to assume spring support system in some nodes along the spline arch to give lateral support effect provided by pre-tensioned membrane. It is also not considered in the model pre-bending stresses produced by initial buckling process needed to get the "elastica" shape in the spline element. Pre-bending stresses and pre-compression ones has been considered in the analysis phase in chapter 3 as additional stresses added to resultant forces acting on the system. The use of some additional vertical truss members to control stability of the system was necessary in order to reduce deformations and to give additional bending stiffness to the arch near from the supports nodes.

It is proposed in this work and erection process sequence.

From the point of view of analysis modeling tools could be improved and a wind tunnel simulation may have been done to evaluate wind effects in a better way and pressure distribution over the surface of the fabric cover. Different heights should be tested to compare behavior results in the analytical model. An experimental program for testing a real scale model must be performed. Finally, a design process must be developed under certain codes and standards to regulate hybrid structures.

### ACKNOWLEDGEMENTS

"The design of a membrane lightweight structure is only governed by forces and imagination, there are no rules, just possibilities"..... (Jürgen Henricke).

I dedicate this work to my parents Eduardo (1945-2006) and Laura because of their huge support and love throughout my life.

Without Lili's support and love, this work would have been impossible to do.

### REFERENCES

- ♦ [1] Adriaenssens S. A. (2000): *Stressed spline structures*. P.H.D. Thesis, University of Bath
- ♦ [2] Adriaenssens S. A. (2008): Feasibility study of medium span spliced spline stressed membranes. In: *International Journal of space structures*. 23 (4), pp. 243-253

# Expanded Applications of High Performance Fiber Rope As Building Structural Members

**Natsuki Yasui<sup>1\*</sup>, Kaidoh Yamaguchi<sup>2</sup>, Osamu Takahashi<sup>3</sup>  
Kaori Tsukano<sup>4</sup>, Yoshinori Tateoka<sup>5</sup>**

<sup>1\*</sup> Dept. of Architecture, Tokyo University of Science, Japan

<sup>2</sup> Dept. of Architecture, Tokyo University of Science, Japan

<sup>3</sup> Dept. of Architecture, Tokyo University of Science, Professor, Japan

<sup>4</sup> Sanwa Tekki Corporation, Japan

<sup>5</sup> Sanwa Tekki Corporation, Japan

**Keywords** – Fiber rope, Seismic brace, Connection fitting, Tension strength, Tensegrity dome, Structural analysis

**Abstract:** A high performance fiber rope made of twisted aramid fibers is lightweight and has high strength in comparison with general structural members such as steel frames. Moreover, this fiber rope is easy to carry because it has high flexibility. In this paper, the following two topics are described to utilize the fiber rope for 'smart' structural members. The first topic is to apply the fiber rope for the seismic brace so that buildings can be easily reinforced in a short period of time. One of important technologies is to connect the fiber rope to the structural members for this application. The connection fitting is studied to sufficiently secure high strength of the fiber rope. Also, points to be noted became clear at the construction stage when the fiber rope is assembled to the connection fitting. The second topic is the structural design and construction of a tensegrity dome using the fiber rope for tension members. This is expected to be used as a framework of temporary space when a disaster occurs. The full size model with 3 meters in diameter is fabricated and then the stress states are analyzed.

## 1. INTRODUCTION

In recent years, demand for high performance fibers has been expanded due to increased global needs for safety and environment issues. The high performance fibers including aramid fiber have excellent properties such as tension strength, heat and chemical resistance, dimensional stability and durability. Thus, the high performance fiber rope have recently been used in many fields such as automobiles, aircraft, and civil constructions.

We have researched and developed on practical technologies in order to apply this high performance fiber rope for building structural members utilizing the above-mentioned features. In this paper, two topics, which include the application for seismic brace and the full size model fabrication of tensegrity dome, are introduced from our various themes regarding to the practical application studies on the high performance fiber rope.

## 2. APPLICATION OF FIBER ROPE FOR SEISMIC BRACE

A reinforcement of building is desired to restrict severe earthquake damage. As shown in fig. 1, it has attempted to apply the high performance fiber rope for the seismic brace so that the building can be easily reinforced in a short period of time. For this application, one of important technologies is to firmly connect the fiber rope to the structural members of the building. We have studied on a connection fitting between the fiber rope and the structural members. Basic requirements of the connection fitting are:

(1) Strength ensure

- To firmly grasp so that the fiber rope does not slip out of the connection fitting.
- To maintain the original strength of the fiber rope in the assembled state.

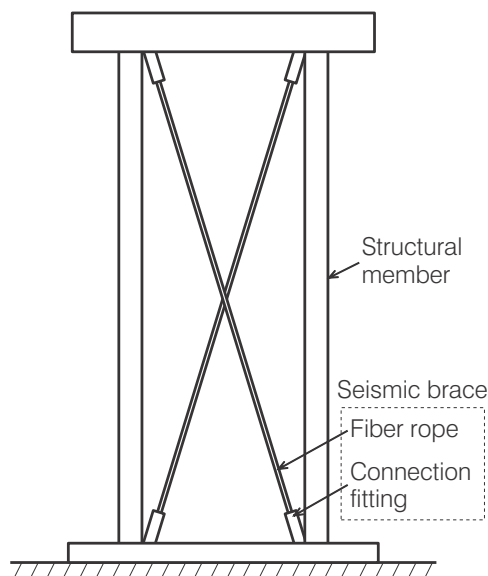


Fig. 1: Configuration of seismic brace using fiber rope

(2) Construction workability

- To easily assemble at the construction site.
- To be lightweight for easy handling.

**2.1. Wedge Type Connection Fitting**

A wedge type connection fitting, which is shown in fig. 2, is selected to prevent that the fiber rope slips off the connection fitting [1][2][3]. For the wedge type connection fitting, the fiber rope is placed between the sleeve and the wedge members of the connection fitting. Then, the fiber rope can be gripped without slippage due to the wedge effect.

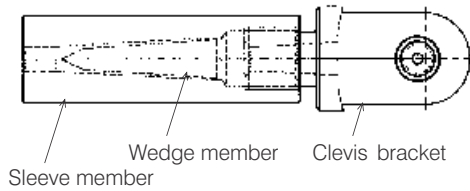


Fig. 2: Configuration of wedge type connection fitting

Tension tests are carried out using three types of fiber ropes with nominal loads of 10 kN, 20 kN, and 50 kN, while assembling them to the wedge type connection fittings [2][3]. The fiber ropes are made of a mixture of p-phenylenediamine (PPD) and 3,4'-diaminodiphenylether (3,4'-ODA), hereinafter referred to 'Technora' [4]. Fig. 3 shows the tension test results and fig. 4 is the break state of the fiber rope. The tension ratio, Rt, indicates a ratio of the assembly breaking load (i.e., the breaking load under the state where the fiber rope is assembled with the connection fitting) against the strength of the fiber rope itself.

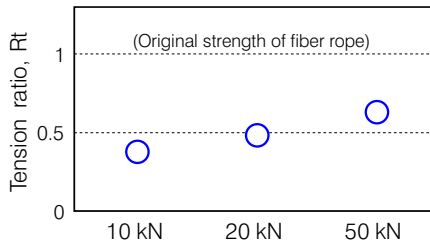


Fig. 3: Tension test results using wedge type connection fitting



Fig. 4: Breaking state of fiber rope

Therefore, 'Rt = 1' means that the assembly breaking load is equal to the original strength of the fiber rope.

The fiber ropes do not slip out of the connection fittings for any cases. However, the fiber ropes are broken around the tip of the wedge members inside the connection fittings. The assembly breaking loads are approximately 50 % of the fiber rope original strength. After analysis, it is found that the fiber ropes are broken due to the stress concentration

around the tip of the wedge members. To improve the assembly breaking loads, it is necessary to reduce the stress concentration in the connection fittings.

**2.2. Optimization of Wedge Shape**

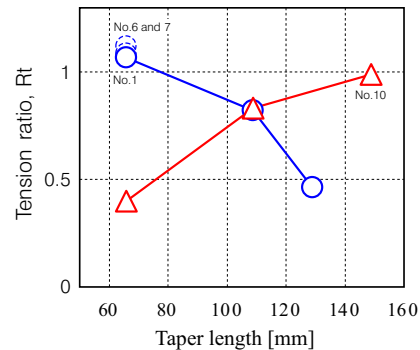
Design studies are made based on experiments to maintain the high strength which the fiber rope itself has [5]. First, the wedge shape (i.e., length and angle of the taper portion) is optimized to improve the stress concentration. For these experiments, the fiber ropes for 50 kN and 100 kN are used. Here, the target is set to break the fiber rope outside the connection fitting (i.e., Rt is close to 1).

Test no.	Nom. rope load [kN]	Consid. item	Wedge		Sleeve		Break load [kN]	Rt [-]	Break. place	
			Taper length [mm]	Taper angle [deg]	Taper length [mm]	Taper angle [deg]				
1	50 (49.4)	---	65.9	3.56	79.5	3.02	52.8	1.07	Outside	
2		Taper length	108.9	3.55	140.0	3.03	40.56	0.82	Inside	
3		Taper length	128.9	3.51	140.0	3.03	22.96	0.47	Inside	
4		Taper angle	65.9	1.65	79.5	1.30	25.52	0.52	Inside	
5		Taper angle	65.9	2.65	79.5	2.09	39.44	0.80	Inside	
6		Confir.	---	65.9	3.56	79.5	3.02	55.3	1.12	Outside
7			---	65.9	3.56	79.5	3.02	53.7	1.09	Outside
8	100 (112.0)	---	65.9	3.78	79.5	3.06	44.6	0.40	Inside	
9		Taper length	108.9	3.34	140.0	3.07	93.2	0.83	Inside	
10		Taper length	148.9	3.36	140.0	3.07	110.9	0.99	Inside	
11		Taper angle	65.9	1.65	79.5	1.08	24.6	0.22	Inside	
12		Taper angle	65.9	2.43	79.5	2.16	70.1	0.63	Inside	

Table 1: Tension test conditions and results

Table 1 summaries the tension test conditions and results. Fig. 5 shows Rt for varied the taper lengths and angles. The 50 kN and 100 kN ropes indicate different tendency. For example, Rt increases according to the increment of the taper length for 100 kN rope while Rt decreases according to the increment of the taper length for the 50 kN rope. This means that there is different optimum condition for each rope.

For the 50 kN rope, the wedge shape under the condition of the test no. 1 satisfies the target. This condition can be optimum for the 50 kN rope. Two additional tests (test no. 6 and no. 7) were conducted under the same condition to eliminate the influence of error and confirm the result. As shown in the dotted circle plots, the rope breakage was confirmed outside the connection fitting for either case.



(1) Varied taperlength

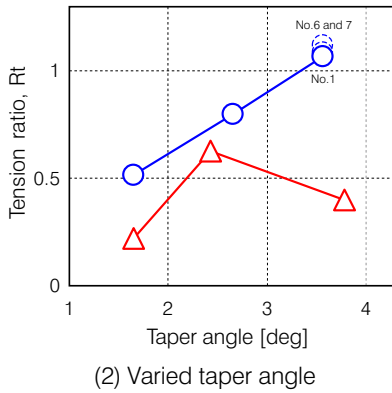


Fig. 5: Tension ratio, Rt, for varied taper lengths and angles

The all 100 kN ropes broke inside the connection fittings. However, the condition of the test no. 10 should be optimum for the 100 kN rope because Rt is closed to 1. Therefore, it is thought that there is a suitable shape of the wedge around this condition.

### 2.3. Surveys on Influence of Assembling Workability

Next, studies on the assembling workability of the fiber rope and connection fitting are described. For the fiber rope, the fibers are twisted into a bundle, and then pluralities of twist bundles are knitted. The fibers are placed around the sleeve hole, and the wedge is driven into the sleeve hole, whereby the fiber rope is assembled to the connection fitting. The influence of fiber rope end treatment when assembling the fiber rope to the connection fitting is investigated. As shown in fig. 6, the following three disengagement states are compared;



Fig. 6: Various disengagement states of fiber rope end

- (1) The state where the fibers are still knitted and twisted, hereinafter referred to 'knitted state'.
- (2) The state where the fibers are not knitted but still twisted, hereinafter referred to 'twisted state'.
- (3) The state where the fibers are completely solved, hereinafter referred to 'solved state'.

Tension test are conducted using the 50 kN rope for investigating the influences of the rope edge treatment. The

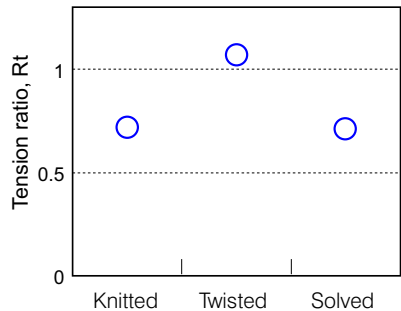


Fig. 7: Influences of fiber rope end treatment

wedge shape of the connection fitting is same as the above-mentioned test no. 1. Fig. 7 shows the results of three different states of the rope edge treatment. The strength under the twisted state is higher than the strength under the solved state. New knowledge that high strength is maintained by leaving the twist of the fiber rope is obtained.

The fiber density should be uniform in the sleeve of the connection fitting. However, there may be unevenness in fibers while assembling. The influence of fiber density deviation when assembling the fiber rope to the connection fitting is also surveyed by comparing the break strengths based on the varied fiber density biases. The rope, which is used for the surveys, consists of 16 bundles of the twisted fibers. The following three cases are tested. Here, the 16 twisted fiber bundles are uniformly or non-uniformly arranged shown in fig. 8.

- (1) The 16 bundles are evenly arranged.
- (2) The 10 bundles are in one side and the 6 bundles are in the other side, hereinafter referred to 'bias 10:6'.
- (3) The 12 bundles are in one side and the 4 bundles are in the other side, hereinafter referred to 'bias 12:4'.

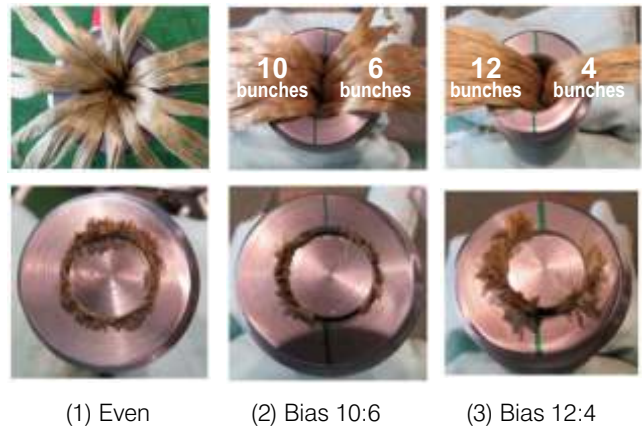


Fig. 8: Various bias states of fiber density

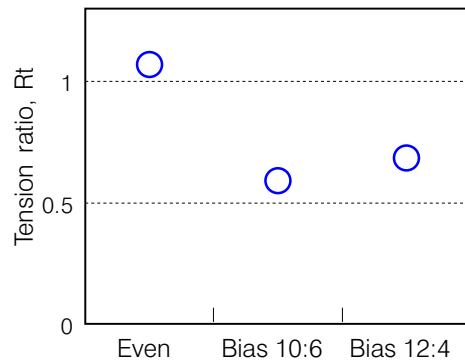


Fig. 9: Influences of fiber density bias

Fig. 9 indicates the results for the fiber density bias. Test conditions are same as the above-mentioned test no. 1. The tension strength decreases when there is a bias in the fiber density. Therefore, for preventing the stress concentration around the wedge member, it is necessary to evenly arrange the fiber rope bundle around the sleeve hole and to accurately drive the wedge member in the center thereof.

## 2.4. Weight Reduction of Connection Fitting

The material of the wedge type connection fitting described above is steel. Aluminum is used to reduce weight of the connection fitting. The friction coefficient of aluminum is lower than the friction coefficient of steel. The fiber rope made of p-phenylene terephthalamide (PPTA), hereinafter referred to 'Twaron', is tested in addition to Technora rope because Twaron rope has the higher friction coefficient compared with Technora rope [4].

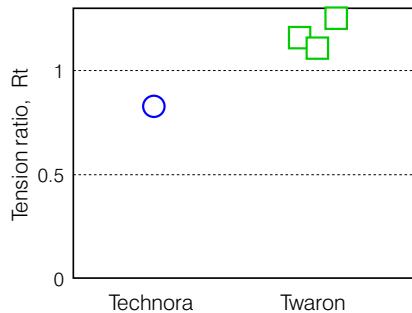


Fig. 10: Tension test results using aluminum fitting

Fig. 10 shows the results for tension tests using the aluminum connection fitting. The test conditions are same as the above-mentioned test no. 1. The fiber rope pulled out of the sleeve member because the friction coefficient was not enough for Technora rope. On the other hand, Twaron rope did not break inside the connection fitting and achieved the target strength. The strength of Twaron rope was confirmed by additional tests. By adopting aluminum for the connection fitting, weight reduction of 77 % in the sleeve portion and 66 % in the wedge portion compared with steel was achieved.

## 3. FULL SIZE MODEL FABRICATION OF TENSEGRITY DOME USING FIBER ROPE

A structural design of the tensegrity dome using the high performance fiber rope is studied through fabricating a full size model. Because only the tensile force (i.e., no bending force) is acted to the members in the tensegrity structure, the entire structure can be simple and lightweight. We have studied that the tensegrity structure can be used for the structural frame of temporary space if a disaster occurs. Since the high performance fiber rope has high tensile strength, it can be used for tension members of the tensegrity structure.

### 3.1. Small Model Fabrication of Tensegrity Dome

The tensegrity structure is composed of isolated compression members which do not contact each other, and tension members which are pulled by the compression members. A systematic structural analysis for utilizing the tensegrity structure has not been established yet. It is necessary that complex geometries and forces of the compression and tension members in the tensegrity structure should be completely controlled to realize the actual dome. Thus, a small model of the tensegrity dome is fabricated to understand its fundamental regularity [6].

The small model of the tensegrity dome consists of

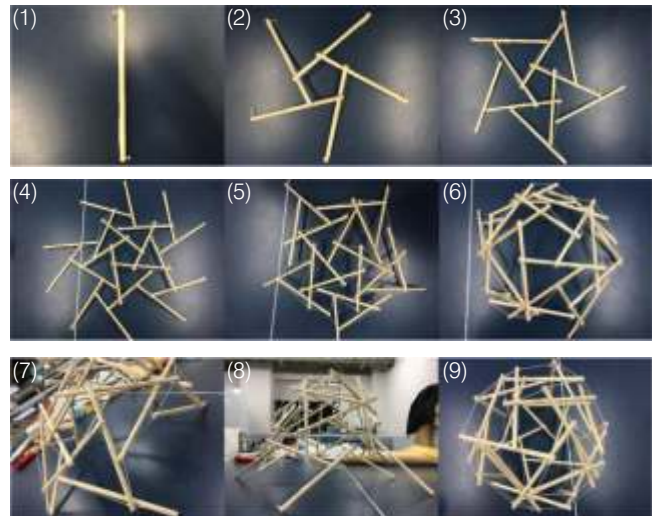


Fig. 11: Fabrication process of small model

wooden struts (as compression members), kite strings (as tension members) and rubber tubes (as connecting members between struts and strings). The wooden struts are 200 mm in length and 8 mm in diameter. Fig. 11 shows fabrication process of the small model.

- (1) Notches of about 5 mm are put at both ends of the strut. The kite strings with appropriate length are fixed at the both ends of the strut as tension members by the rubber tubes.
- (2) One end of the other strut is connected to the approximately one-third position in the strut length. Then, a pentagon shape is formed by connecting the five struts.
- (3) A triangle shape is formed by the other end portions of the five struts.
- (4)(5) The pentagon and triangle shape are alternately fabricated by repeating the above-mentioned processes.
- (6)(7)(8) The struts start to stand after the forces are applied to the tension members. The struts are added one after the other.
- (9) The last pentagon is formed and the tensegrity dome is completed. The 30 compression members and the 30 tension members are used for the tensegrity dome, respectively.

The following points were found out through the fabrication of this small model.

- Although each member can be easily connected, the position and direction of the members are complicated. Thus, they should be carefully considered.
- The dome remains flat until the tension actually occurs. Then, the dome gradually becomes three-dimensional as the tension increases.
- The dimensional accuracy of the kite strings (i.e., tension members) is very important for fabricating the tensegrity dome. Thus, the connection members which

can adjust the length of the tension members are definitely needed. Also, the connection members are required to reduce the twist of the tension members.

### 3.2. Fabrication of Full Size Model

Based on the experiences obtained from the small dome model, a real size model (about 3 meters in diameter) of the tensegrity dome is fabricated. A plastic pipe (length 2000 mm, outside diameter 32 mm, inside diameter 25 mm) is used for the compression member, a fiber rope (diameter 4 mm) is used for the tension member, and a pipe cap (inside diameter 32 mm) is used for the connection member, respectively. The plastic pipe is made of polyvinyl chloride and the material of the fiber rope is the above-mentioned Technora. Since the high performance fiber rope is used as the tension members, the dome can be constituted by thin ropes. Fig. 12 is a conceptual drawing of the full size model.

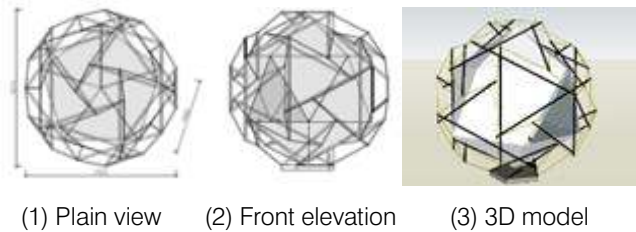


Fig. 12: Conceptual drawing

Fig. 13 shows the full size model and its fabricating scene. Theoretically, there are no bending forces acted to the compression members in the tensegrity structure. Since the length accuracy of the tension members is insufficient, however, the length errors are absorbed by the bending of the compression members. The dimensional shapes of the tensegrity dome are roughly confirmed for structural analysis on the basis of the full size model.



Fig. 13: Full size model and its fabricating scene

### 3.3. Structural Analysis

As can be seen from the fabrication of the small model, the tensegrity dome does not stand when no tension is applied to the tension members. The dome height gradually increases as the tension force increases. Since the forces acting to the compression and tension members change

complicatedly, no commercial software is available at present to express and analyze this dynamic behavior. For the first step, static structural analysis is carried out based on the fabricated full size model. Elastic analysis is performed using general-purpose structural analysis software. Table 2 shows the specifications of each member used for the structural analysis. The modeling outline is as the follows.

- The members are modeled as common beam elements. The analysis model has 120 elements and 60 nodes.
- The fulcrums are assumed to be pin support. That is, the movement of the fulcrums is fixed in the vertical and horizontal directions but can freely be rotated.
- The nodes in the tensegrity dome are considered to be semi-rigid joints. Therefore, the fiber rope characteristics are approximated by assuming the nodes to be rigid and multiplying the second area moment about Y and Z axis by 0.1 in the section modulus.
- Linear analysis is used for the structural analysis of the tensegrity dome since it is designed within the elastic behavior range.

Compression member (Plastic pipe)	Elastic modulus	$2.80 \times 10^3 \text{ N/mm}^2$
	Poisson coefficient	0.38
	Relative density	$1.40 \times 10^{-5} \text{ N/mm}^3$
Tension member (Fiber rope)	Elastic modulus	$7.25 \times 10^4 \text{ N/mm}^2$
	Poisson coefficient	0.30
	Relative density	$1.39 \times 10^{-5} \text{ N/mm}^3$

Table 2: Specifications of structural members

Each condition for structural analysis is based on Article 82 of the Enforcement Ordinance of Construction Standard Law of Japan. As examples of the structural analysis, two cases such as the short-term seismic load and the short-term wind load are introduced.

Fig. 14 shows a stress diagram in X direction for the short-term seismic load as the example of the analysis result. Here, the short-term seismic load is 0.2 G based on the architectural primary design. Table 3 summarizes the analysis results for the short-term seismic load. The check value, which is a ratio between the maximum and criteria stresses, indicates the margin against the material strength. It was confirmed that the maximum tension and compression stresses are less than the allowable stress, respectively.

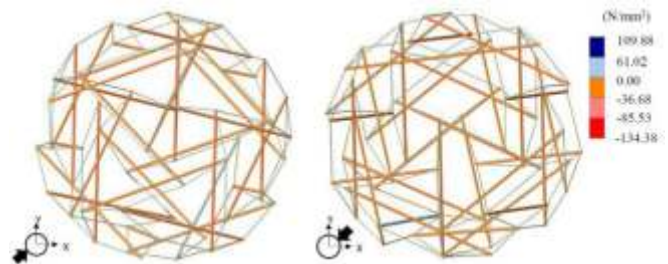


Fig. 14: Stress diagram in X direction for short-term seismic load

Member	Direction	Maximum stress (N/mm <sup>2</sup> )	Criteria stress (N/mm <sup>2</sup> )	Check value
Compression member (Plastic pipe)	X direction	7.37	62.00 (Com.)	0.119
	Y direction	6.96		0.112
	45 deg. direc.	7.47		0.120
Tension member (Fiber rope)	X direction	109.88	3470.00 (Ten.)	0.032
	Y direction	96.43		0.028
	45 deg. direc.	94.34		0.027

Table 3: Analysis results for short-term seismic load

As the example of the analysis result for the short-term wind load, fig. 15 is the stress diagram in the X direction. The wind load is assumed to be  $3.05 \times 10^2$  N. Table 4 shows the analysis results for the short-term wind load. Similarly, it was verified that the maximum tension and compression stresses are within the allowable stress range for the short-term wind load.

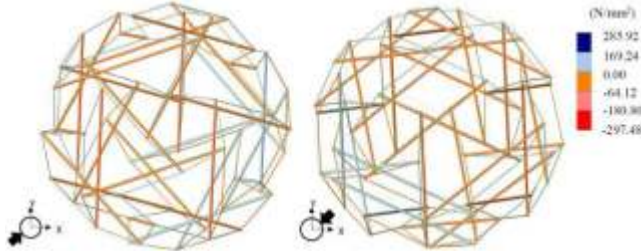


Fig. 15: Stress diagram in the X direction for short-term wind load

Member	Direction	Maximum stress (N/mm <sup>2</sup> )	Criteria stress (N/mm <sup>2</sup> )	Check value
Compression member (Plastic pipe)	X direction	8.89	62.00 (Com.)	0.143
	Y direction	9.22		0.149
Tension member (Fiber rope)	X direction	282.18	3470.00 (Ten.)	0.081
	Y direction	96.43		0.028

Table 4: Analysis results for short-term wind load

#### 4. SUMMARY

The following conclusions were obtained through the researches for applying the high performance fiber rope as building structural members by utilizing their flexibility with high strength.

First, the wedge type fitting for connecting the fiber rope to the structural members was examined through experiments. This connection fitting is aimed at the practical application for the seismic brace which can be constructed easily at the construction site. The appropriate connection fitting, which can sufficiently secure the fiber rope strength, was obtained by optimizing the wedge shape of the fitting. The points to be noted at the construction stage (e.g., the

rope end treatment) were also clarified. Furthermore, weight reduction was achieved by adopting aluminum for the connection fitting instead of steel.

For the future researches on the connection fitting, a suitable value of the wedge shape for the 100 kN rope is surveyed. Then, the high performance fiber rope will be tried to apply for actual buildings to improve the seismic resistant strength.

Second, the tensegrity dome using the high performance fiber rope was studied to expand its application range for building structural members. This tensegrity dome is expected to be used as frames of the temporary space at the time of disaster occurrence. After obtaining the knowledge on the tensegrity dome by making the small model, the full size model with a diameter of about 3 meters was fabricated based on this knowledge. Furthermore, it was confirmed that each structural member was within the allowable stress range through the static structural analysis based on the fabricated dome model.

For the future researches on the tensegrity dome, the forces acting on each structural member are examined and the consistency with the analysis model is confirmed. Then, the accuracy of the structural analysis method for the tensegrity dome can be improved. Also, the connection fitting may be developed to easily and accurately adjust the length of the fiber rope as the tension members.

#### REFERENCES

- [1] Takahashi, O., Yamaguchi, K., Hiramoto, T., Yokoyama, A., Maeda, H., Tateoka, Y., "Study on Application to Structural Members of High-Performance Fibers, Part 1: Development Outline", Proceedings of Architectural Institute of Japan, 2016
- [2] Yamaguchi, K., Takahashi, O., Hiramoto, T., Yokoyama, A., Maeda, H., Tateoka, Y., "Study on Application to Structural Members of High-Performance Fibers, Part 2: Performance Characteristic Test (Wooden Frame)", Proceedings of Architectural Institute of Japan, 2016
- [3] Yamaguchi, K., Takahashi, O., Tateoka, Y., "Research and Development on Brace Members Using High-Performance Fibers", No. C1-67, 6th ASIA Conference on Earthquake Engineering (6ACEE), 2016
- [4] Homepage of Teijin Limited, February 20, 2017, <<https://www.teijin.co.jp/>>
- [5] Yasui, N., Yamaguchi, K., Takahashi, O., Tsukano, K., Tateoka, Y., "Study on Application of High Performance Fiber for Structural Members, Part 3: Consideration of Wedge Type Connection Fitting", Proceedings of Architectural Institute of Japan, 2017
- [6] Ishida, D., Kato, K., "Study on Structural Character and Construction on Tensegrity Sphere", Proceedings of Toyota National College of Technology, 2009



# Structural Design of a Seismic Isolated Building in Matsumoto City, Japan

Yuki Nagai<sup>1\*</sup>, Toshiaki Kimura<sup>1</sup>, Musturo Sasaki<sup>2</sup>

<sup>1\*</sup> Sasaki Structural Consultants, Engineer, Japan

<sup>2</sup> Sasaki Structural Consultants, President, Japan

**Abstract:** A new building of a newspaper company which is under construction and designed by “TOYO ITO & ASSOCIATES, ARCHITECTS” has been planned in Matsumoto-city, Nagano Prefecture, Japan.

This paper reports about a structural design and a seismic isolated design of this project. This building was required to be able to use in an emergency such as an earthquake as a newspaper company, and to be able to provide the function of a refuge place for the citizens. From this point of view, the basic concept of the structure of this building was set as below;

- For the high aseismic performance requirements, the rigid frame structure which is consisted by the concrete filled steel pipe column (CFT) and H-section beam, and the seismic isolation dumper were adopted.
- The floor steel girder is designed with “Grid-girder” to provide excellent degree of freedom and future updating property for comfortability for interior space.

First, this paper describes about the architectural plan. Next, structural planning with respect to mainly seismic isolation structure is explained. After explanation of the structural planning, the detail of the structural design (verification by using time history response analysis) is shown.

## 1. INTRODUCTION

A new building of a newspaper company which is under construction and designed by “TOYO ITO & ASSOCIATES, ARCHITECTS” has been planned in Matsumoto-city, Nagano Prefecture, Japan. The site is on the center of the city area and there are the commercial buildings and the cultural buildings around the site. On the other hand, there is also rich nature such as rivers flowing around there.

This new building has about 8000 square meter total floor area, and about 24 meter height. It has 5 stories above ground and one below; the commercial complex such as a gallery, a community hall, a restaurant and a shop, are located on the first floor to the third floor. The business area for the newspaper company is located on the fourth and fifth floor. A parking lot is located on the basement floor.

## 2. STRUCTURAL PLANNING

### 2.1 Overall

This building contains an office building of a newspaper



Fig. 1: Image of building (Image by “kuramochi + oguma”)

company that provides information for citizens in this area, and a commercial complex that citizens can use. At the same time, it was required to be able to use in an emergency such as an earthquake as a newspaper company, and to be able to provide the function of a refuge place for the citizens. From this point of view, the basic concept of the structure of this building was set as below;

- For the high aseismic performance requirements, the rigid frame structure which is consisted by the concrete filled steel pipe column (CFT) and Hsection beam, and the seismic isolation dumper were adopted.
- The floor steel girder is designed with “Gridgirder” to provide excellent degree of freedom and future updating property for comfortability for interior space.

### 2.2 Super Structure

This super structure is basically designed with the rigid frame system of 15.6m span on demand from building use. The CFT columns, which diameter is 850mm in the first floor and 750mm in the second to fifth floor, are arranged every 15.6m as main frame structure, and the  $\phi 450$  steel pipe columns are arranged on the front side of the building. The main girder for the rigid frame is 900mm height H-section steel beams. The floor steel girder is the grid-girder to distribute vertical load in two directions, which transfer the large-span floor load in a rational way.

The rigid frames of the upper structure possess enough rigidity and strength for wind load and seismic load, while achieving the universal-space for building use and open-

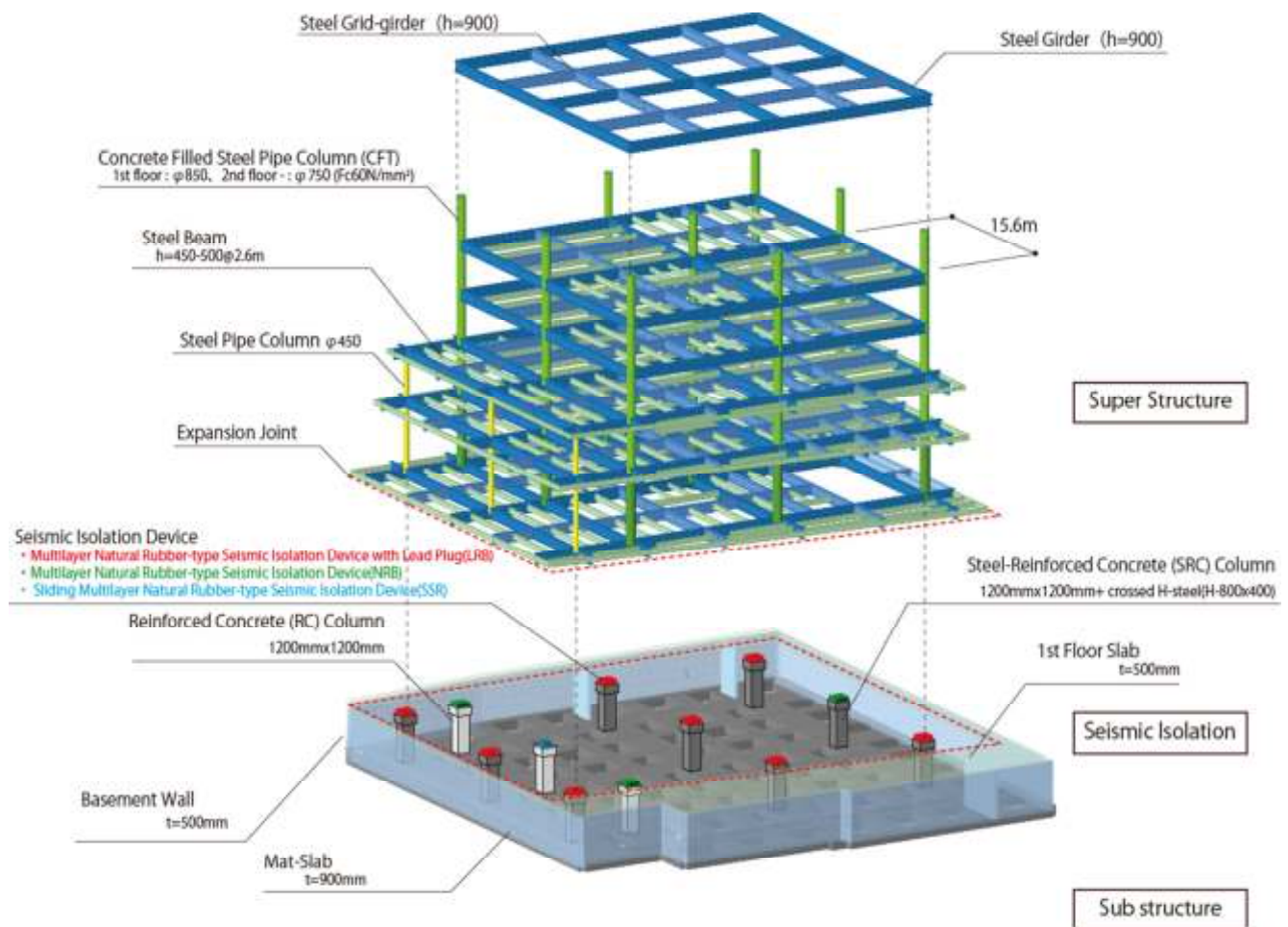


Fig 2. Structural Diagram elevation to the city.

### 2.3 Seismic Isolation

The economic steel rigid-frame and excellent earthquake resistance performance are enabled by the deployment of seismic isolation dampers that absorb significant amount of incoming seismic forces. Seismic isolation device is installed in the position of the capital part of the column on the first basement floor. Three types of the seismic isolation damper were used depending on the performance required for the earthquake resistance as follows;

- Multilayer Natural Rubber-type Seismic Isolation Device with Lead Plug
- Multilayer Natural Rubber-type Seismic Isolation Device
- Sliding Multilayer Natural Rubber-type Seismic Isolation Device

The seismic force from super structure is transferred to the cantilever RC and SRC column through the seismic isolation damper. The arrangement of the columns was determined according to the magnitude of the shear force.

With the assumption which the super structure behave as the rigid body and the columns under the seismic isolation do not significantly affect the natural period of the whole structure, the layout of the seismic isolation device is

arranged by using following scheme;

- (1) Mass above the seismic isolation layer, equivalent stiffness and equivalent damping factor of the seismic isolation layer derived from the horizontal displacement based on the shear strain (10-200%) are set.
- (2) Based on equivalent stiffness and equivalent damping factor of the seismic isolation device which shear strain is reached 10-200%, one-dimensional response spectrum analyses by using some strong ground motion are implemented and the response of acceleration and displacement are calculated.
- (3) By using the maximum acceleration and seismic shear distribution coefficient ( $A_i$  distribution in JPN design-code), the static force is calculated, and static analysis is implemented.
- (4) Through (3), if there is no satisfaction of the criteria, the arrangement of the seismic isolation is modified, and return to (1).

The basic image of the scheme is drawn in Figure3. and Figure4 represents the final arrangement of the seismic isolation. It can be confirmed that by using scheme, the arrangement of the seismic isolation device which can be satisfied with a certain criteria can be easily derived.

## 2.4 Sub Structure

The lower structure for machine room and parking lots is mainly designed with concrete. Considering the high groundwater level, the lower structures are designed with 900mm height flat RC slabs in order to minimize the volumes of the ground excavation. This slab resists to buoyancy force and bending force acting on the RC and SRC column base.

Owing to its ground condition, the foundations are designed as cast-in-place steel pipe concrete pile supported by gravel layer located at about twenty meters below ground.

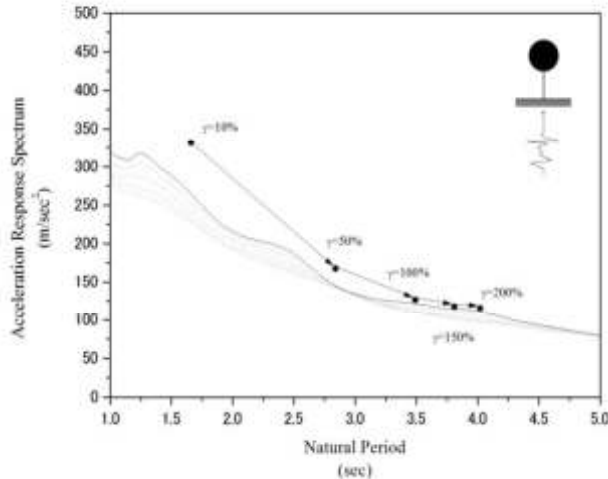


Fig. 3: The basic image of the scheme

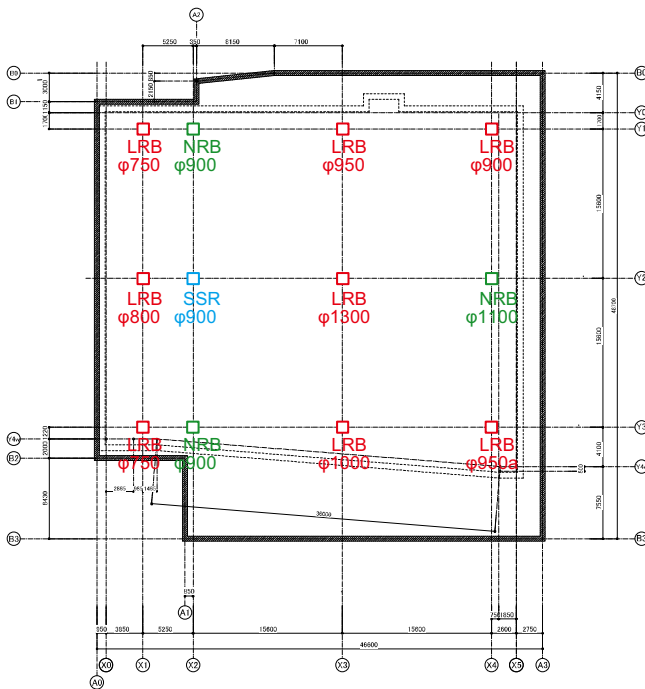


Fig. 4: The final arrangement of the seismic isolation

## 3. STRUCTURAL DESIGN FOR SEISMIC FORCE

### 3.1 Abstract

For the verification of structural safety of this building,

time historical response analysis is implemented. Two kinds of ground motion (one is named “Level1” and assumed a return period of 50 years, the other is “Level2” and a return period of 500 years) are set for the input of this verification. Moreover, based on the result against “Level 2” ground motion, the margin of the structural capacity against larger earthquake is also checked. The criteria of this building (with respect to the super structure and the layer of the seismic isolation) are shown in Figure 5.

### 3.2 Analytical model

For the purpose of achieving compatibility between simplification and the check of three-dimensional behavior, the super structure is dealt with three-dimensional shear model which has mass considered about moment inertia and shear stiffness included torsion rigidity. And, as the lower structure, the column which supports the seismic isolation device is dealt with 3D beam element. The seismic isolation devices are dealt as linear or nonlinear spring, and the bottom of the column in the lower structure is supported as fixed support.

Figure 6 represents the image of the analytical model and the characteristic of restoring force with respect to the seismic isolation (overall) is shown in Figure 7. About ground motion for the input, Figure 8 represents the pseudo velocity response spectrum. Furthermore, in numerical analysis against “Level 2” ground motion, some case is provided for the consideration the effect with respect to the variation of shear stiffness caused by product error, secular change of the seismic isolation device and environmental temperature. Analytical cases are shown in Figure 9.

Index		Level1	Level2
Super Structure	Stress	Elastic	Elastic / Elastic limit <sup>*1</sup>
	Drift angle	1/200	
Seismic Isolation	Disp.	40cm	
	Shear Strain	200%	
	Surface Pressure (+) <sup>*2</sup>	Under stable deformation	
	Surface Pressure (-) <sup>*3</sup>	No tensile stress	

\*1: In the case which is considered the variation of shear stiffness caused by product error, secular change of the seismic isolation device and environmental temperature.

\*2: Represents compression stress.

\*3: Represents tensile stress.

Fig. 5: Design Criteria

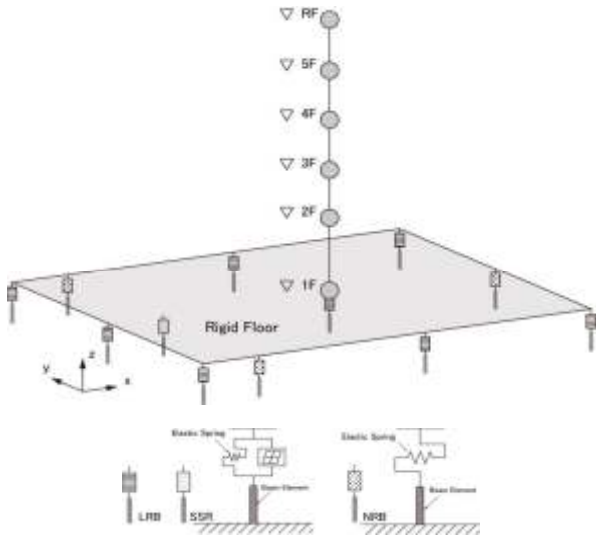


Fig. 6: Analytical model

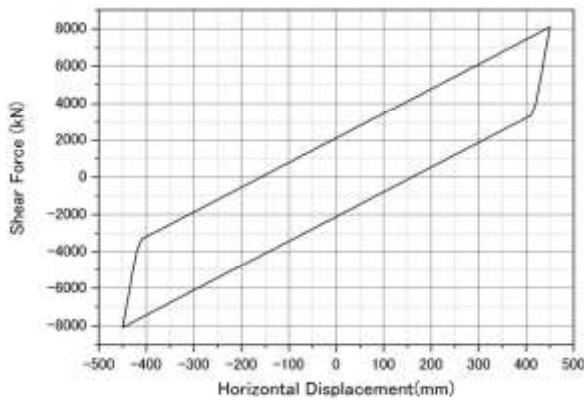


Fig. 7: Restoring force with respect to the seismic isolation

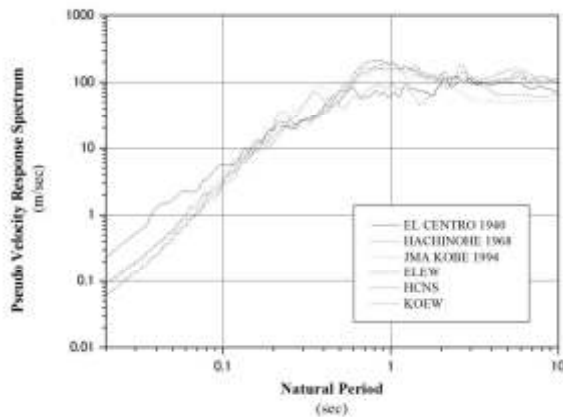


Fig. 8: Pseudo velocity response spectrum

No	Name of the Numerical case	the variation of shear stiffness
1	Case-N	Not consider
2	Case-H	Consider increase
3	Case-S	Consider reduction

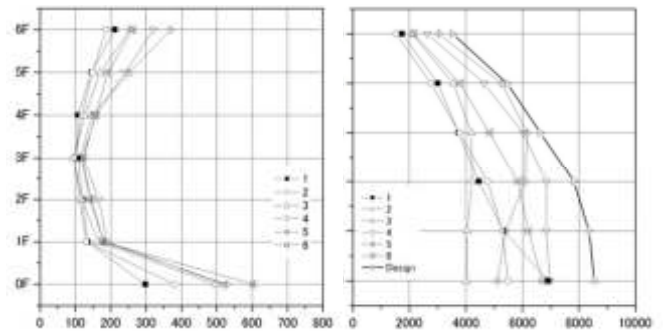
Fig. 9: Design Criteria

### 3.3 Result

The result of Case-N is shown in Figure 10, where the maximum of the response acceleration, lateral force and horizontal displacement at each floor are represented. It can be confirmed that each structural member has elastic state, the maximum of the horizontal displacement and drift angle are not exceeded the criteria and the maximum displacement of the seismic isolation layer is under 400mm which is equivalent to maximum of shear strain (200%) with respect to seismic isolation device. And from results of Case-H and Case-S, which are shown in Figure 11 and 12, it can be confirmed that the structure is satisfied with design criteria regardless of the variation of shear stiffness of the seismic isolation device. And from the series of such result, it is useful to be point out that the building has appropriate seismic safety against the strong ground motion.

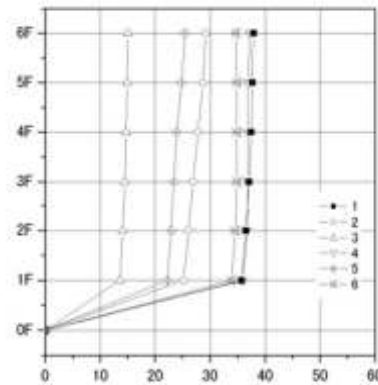
### 4. DETAIL DESIGN

Figure 13 shows the example of detail design around the seismic isolation device. Seismic forces are translated to the main frame through the steel base plate and the rib plate above and below the seismic isolation device. In addition, the foundations of concrete are arranged as the fire-resistive covering of seismic isolation equipment. The SRC (RC) Column resists the bending moment and shear force from the seismic isolation device and these forces are transferred to the mat-slab.



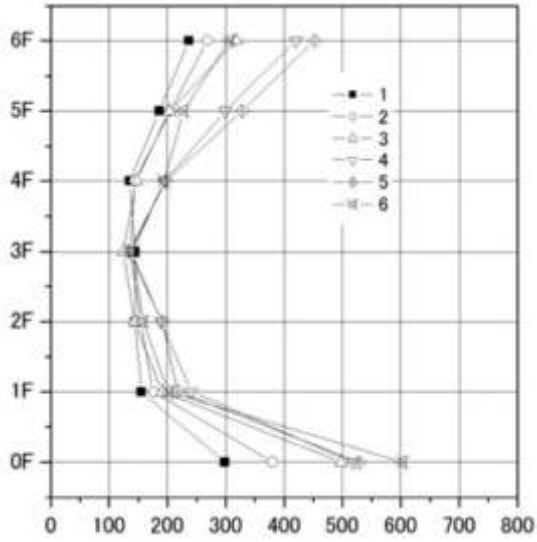
[1] Acceleration(cm/sec<sup>2</sup>)

[2] Static shear force(kN)

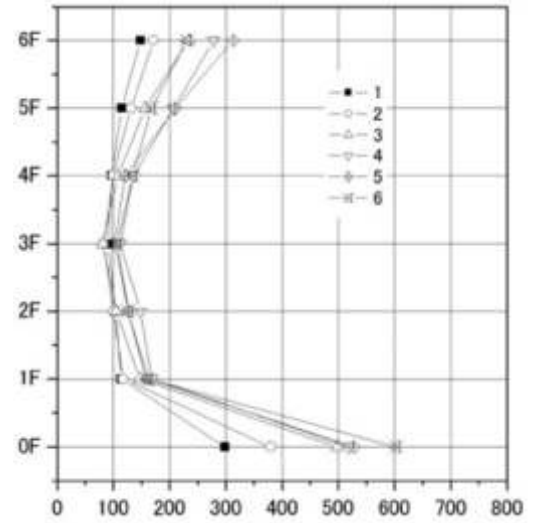


[3] Horizontal displacement(cm)

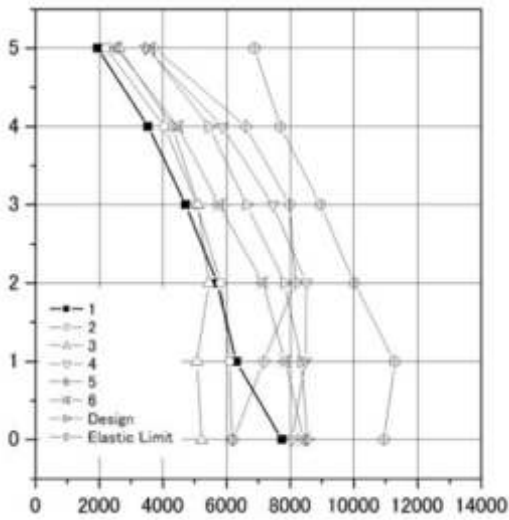
Fig 10: The result of Case-N



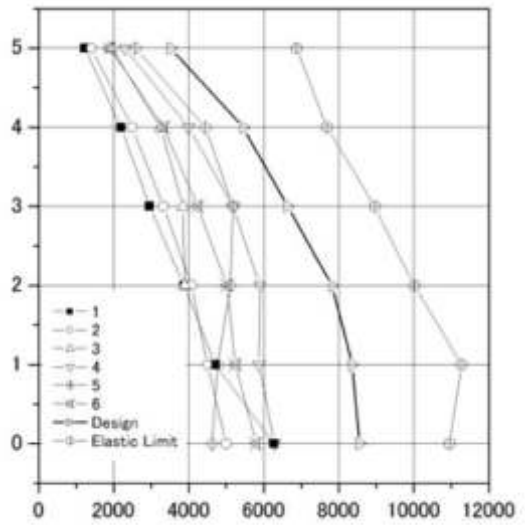
[1] Acceleration(cm/sec<sup>2</sup>)



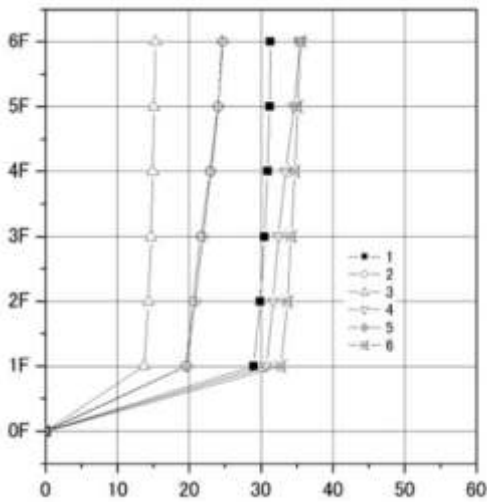
[1] Acceleration(cm/sec<sup>2</sup>)



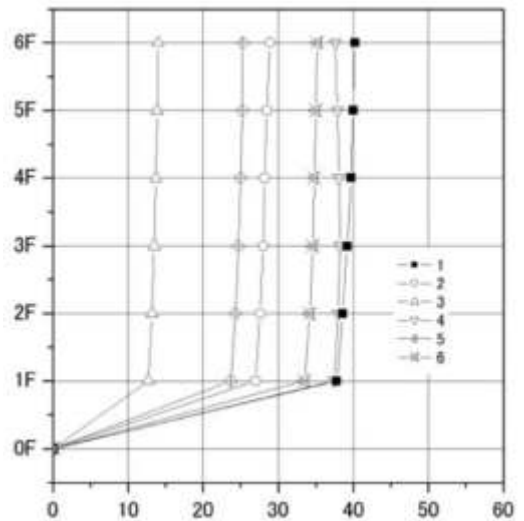
[2] Static shear force(kN)



[2] Static shear force(kN)



[3] Horizontal displacement(cm)



[3] Horizontal displacement(cm)

Fig 11: The result of Case-H

Fig 12: The result of Case-S

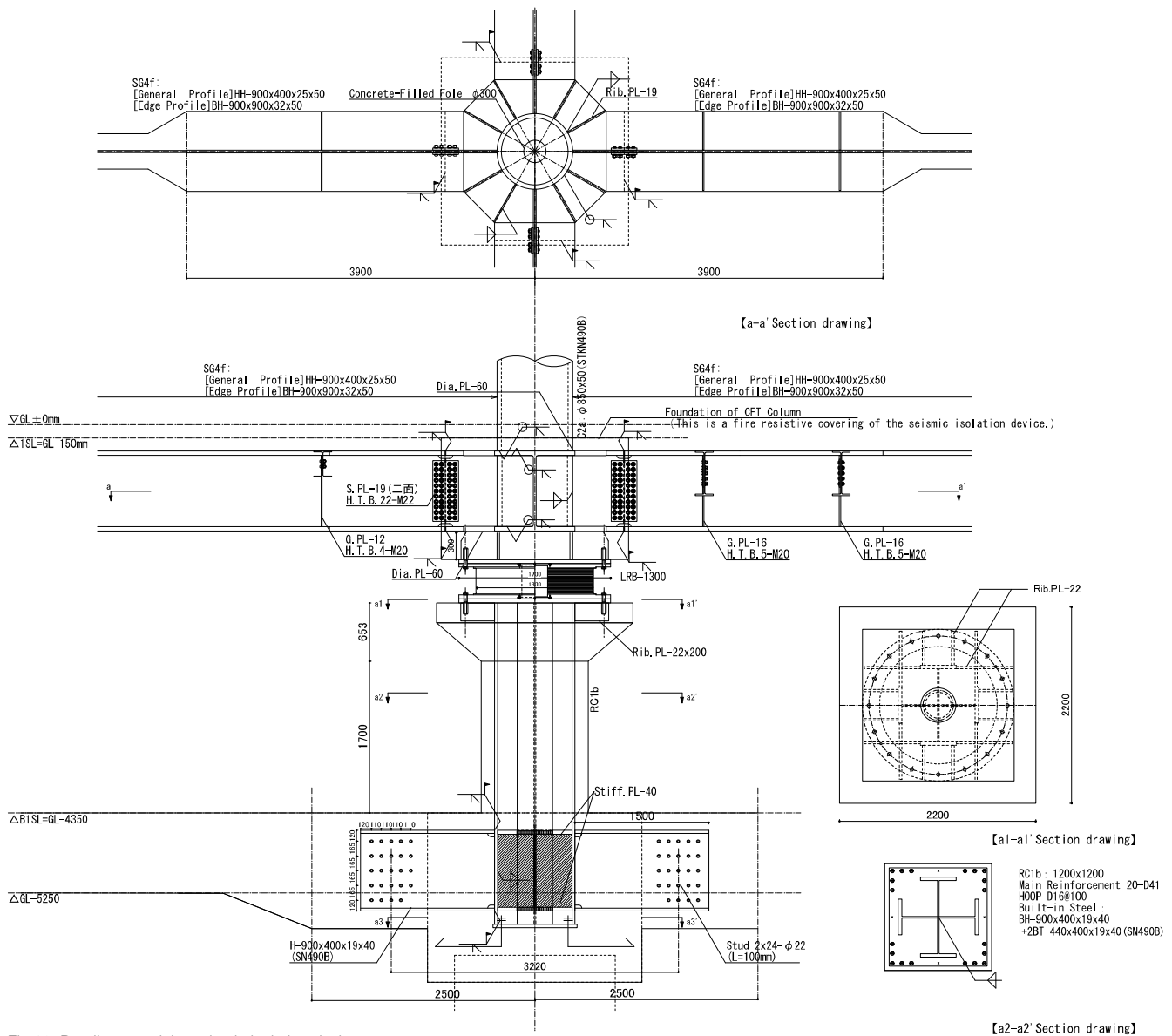


Fig 13: Details around the seismic isolation device

## 5. CONCLUSION

This paper reports about the under construction project of seismic isolated building. The essentials presented in this paper can be summarized as follows,

- This paper focuses on a new building of a newspaper company which is under construction and designed by “TOYO ITO & ASSOCIATES, ARCHITECTS” has been planned in Matsumoto- city, Nagano Prefecture, Japan. And the abstract of the architectural planning, structural planning and structural design are reported.
- With respect to the structural planning, by using reported scheme, it can be confirmed that the arrange-

ment of the seismic isolation device which can be satisfied with a certain criteria can be easily derived.

- With respect to verification of seismic safety in the structural design, it can be confirmed that the structure is satisfied with design criteria regardless of the variation of shear stiffness of the seismic isolation device, and it is useful to be point out that the building has appropriate seismic safety against the strong ground motion.

## ACKNOWLEDGEMENTS

The authors would like to thank “TOYO ITO & ASSOCIATES, ARCHITECTS” for providing us the building information and so on.

# Pedestrianisation of Meenakshi Temple Surrounds

**Ar. Valliappan Ramanathan**  
Principal Architect, Karvin Design Studio, India

**Abstract:** Madurai, one of the oldest cities in Tamil Nadu, is famous for its rich heritage and cultural history. The Madurai Meenakshi Amman temple is one of the most important landmarks in the city. Due to rapid urbanization, the area surrounding the temple began facing issues due to increased density and congestion.

Ar. Valliappan Ramanathan, Principal Architect and Urban Designer, Karvin Design Studio, was appointed as the urban design consultant by the Madurai city corporation to relieve the city centre of pressure for space and infrastructure.

Under JnNURM scheme, a Detailed Project Report on heritage sites of the Madurai city was prepared by Karvin Design Studio. In this DPR, after a detailed study various proposals for the heritage sites were submitted. One such proposal was that of converting the Chithirai veedhi, the street encircling the temple quadrilateral into a pedestrian zone. Thus was born the idea of pedestrianisation in the region.

## 1. INTRODUCTION

One of South India's great temple towns, Madurai is synonymous with the celebrated Meenakshi Temple. Situated on the banks of river Vaigai, Madurai has a rich cultural heritage passed on from the great Tamil era more than 2500 years old.

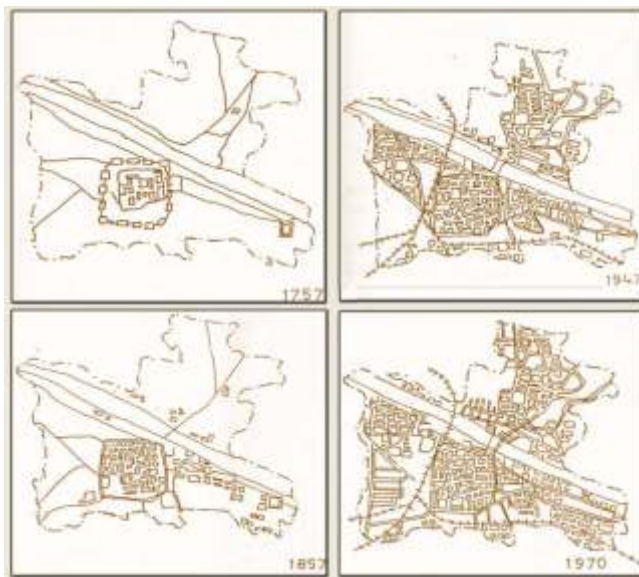


Fig. 1.1: Evolution of Madurai city

Meenakshi Sundareswarar twin Temple is the pivot around which the entire city has evolved. The Meenakshi Temple complex is literally a city - one of the largest of its kind in India and undoubtedly one of the oldest too. The temple grew with the contribution of each dynasty and victorious monarchs, into an enormous complex extending over an area of 65000 Sq m.



Fig. 1.2: Aerial view of Meenakshi temple.

Lord Siva in his incarnation as Sundareswarar and his fish-eyed spouse, Meenakshi, are enshrined in this twin temple. There are four massive gateways enclosing these two shrines. Even a casual visitor is fascinated by the city's rich cultural heritage and its colourful festivals.



Fig. 1.3: Temple Car Festival during Chitrai Festival

## 2. BACKGROUND

Due to rapid urbanization, the area surrounding the temple began facing issues due to increased density and congestion. The Madurai City Corporation wanted to relieve the centre of the pressure for space and infrastructure. In the year 2004, the Madurai City Corporation and the district administration wanted to spruce up the Meenakshi Temple surrounds. Initially, the city authorities came up with the idea of laying a concrete road around the temple precinct.

Our firm being actively involved in such public designs, vehemently objected such piecemeal solutions. After several rounds of awareness meetings with the authorities a formal work order was given to our firm for a comprehensive design scheme of “Beautification of the Meenakshi Temple surrounds”.

A thorough study of the precinct and the core city was carried out by our firm and a detailed proposal with immediate action plans and long term plans were proposed.

Subsequently, under Jawaharlal Nehru National Urban Renewal Mission (JnNURM) Scheme which was a massive city-modernization scheme launched by the Government of India under Ministry of Urban Development, our firm was awarded the scope of “Preparation of heritage DPR” for Madurai.

## 3. IDENTIFICATION OF CULTURAL AND HERITAGE ZONES

For the purpose of categorical listing of the heritage sites, the following 4 preservation zones had been proposed.

**ZONE A:** The originally planned town around Sri Meenakshi Amman Temple is the most important from heritage point of view. There are a large number of religious and cultural buildings in this precinct.

**ZONE B:** This area in Tallakulam includes besides Perumal Temple and its open space, other buildings and areas of cultural and heritage importance such as Gandhi museum, Tamukkam exhibition ground, Rajaji Park, and American college.

**ZONE C:** The famous Mariamman Teppakulam at Vandiyoor with its surrounding area has been identified as

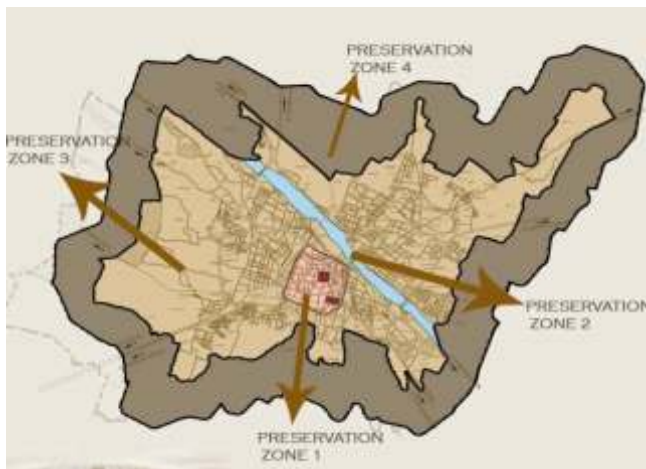


Fig. 3.1: Heritage Zones – Madurai Corporation limit

cultural and heritage zone ‘C’. The zone also includes important choultries.

**ZONE D:** This zone incorporates identified heritage spots outside the Madurai corporation limits.

## 4. CHARACTERISTICS OF HERITAGE ZONE A: CORE CITY

According to legend, Viswanatha Naicker, was the architect to plan the city in the form we see today. The primary characteristics of the core city are:

- Highly ritualistic
- Rapidly commercializing
- Ironically a unique mix of culture and commerce
- Encroached pedestrian pavements
- Endangered survival for inhabitants and visitors
- Commodities inflow and out flow
- Traffic menace
- Insufficient parking facilities
- Lacuna of pilgrim/tourist amenities
- Lacuna of appropriate bye laws

## 5. CORE CITY ISSUES

A comprehensive study and analysis lead to the identification of the following core city issues.

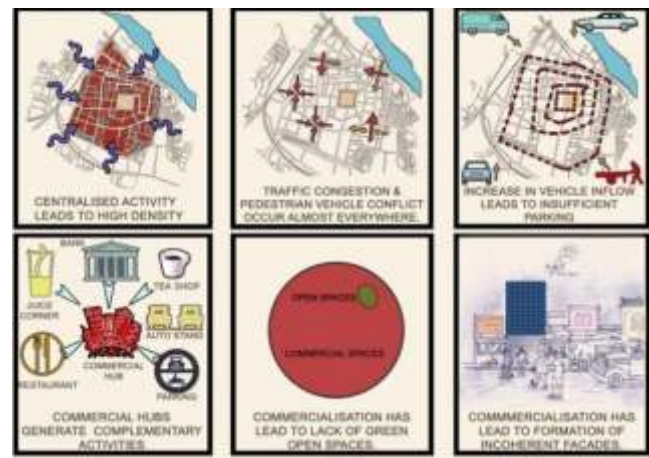


Fig. 5.1: Core city issues



Fig. 5.2: Core city issues



Centralized activity had lead to increase in traffic congestion and pedestrian vehicle conflict. Simultaneously rapid commercialization had also lead to lack of green spaces and formation of incoherent facades and all the above core city issues.

### 6. CORE CITY POTENTIALS



Fig. 6.1: Core city potentials

With a globally renowned Heritage complex at the core and heritage monuments scattered around the town, and well linked by air, rail, and air, the urban fabric owns a very high potential for development as represented above.

### 7. ACTION PLANS

As an outcome of the above detailed study of the core city issues and potentials, the following action plans were proposed.

#### IMMEDIATE ACTION PLANS:

- Listing and integrating the heritage spots of the city. Creating public awareness about heritage conservation.
- Stringent laws to prevent additional commercial activity in the heritage core.
- Relocating corporation and other encroached shops around heritage precincts including shifting of the old central vegetable market outside the core.

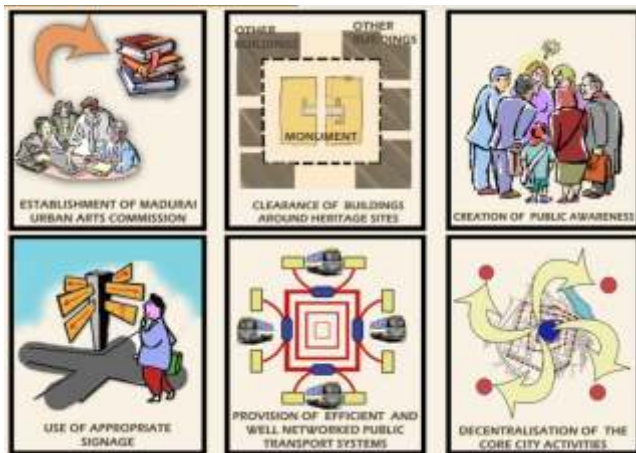


Fig. 7.1: Core city- Action plans

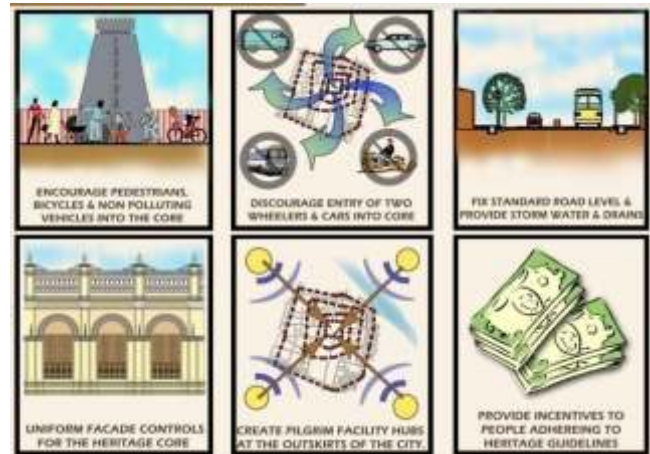


Fig. 7.2: Core city- Action plans

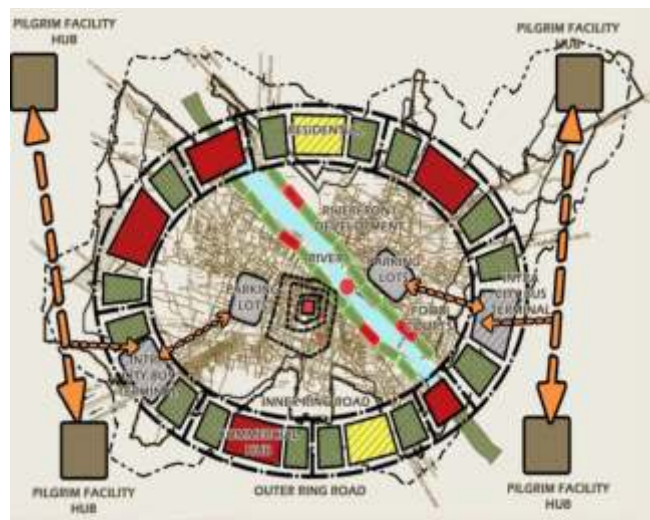
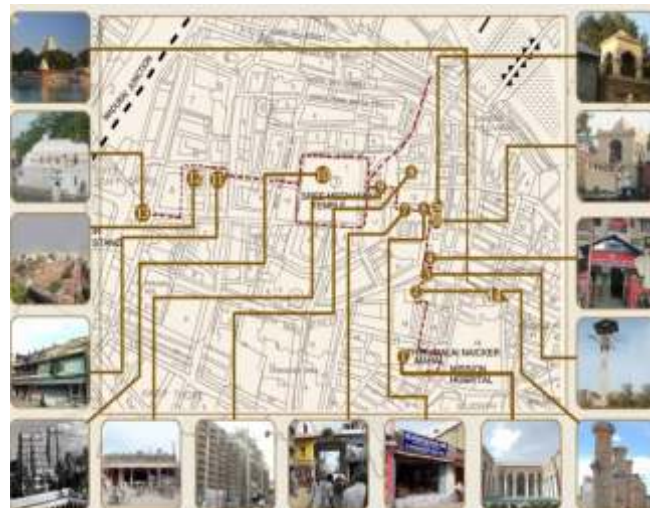


Fig. 7.3: Proposed structural plan



- 1.Thirumalai nayak palace
- 2.Pattuthoon
- 3.Vilakkuthoon
- 4.Vilakkuthoon Police Station
- 5a.Amman Thermutti
- 5b.Swami Thermutti
- 6.Press
- 7.Vittavasa
- 8.Raya Gopuram
- 9.Pudumandapam
- 10.Meenakshi Temple
- 11.Ganshi Ninaivigam
- 12.Perumal Kovil Tank
- 13.Fort wall
- 14.Mariamman temple tank

Fig. 7.4: Heritage spots in Madurai

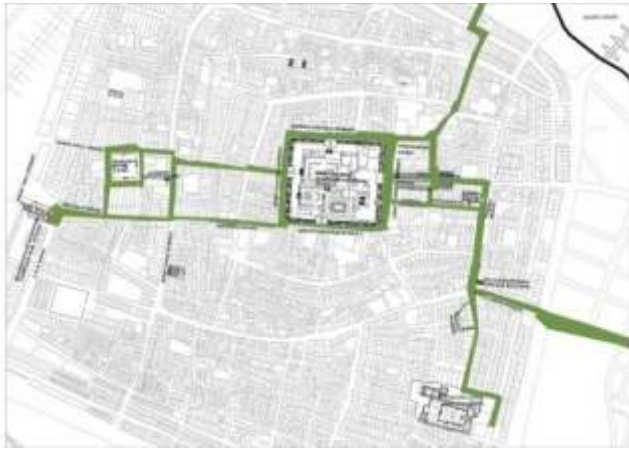


Fig. 7.5: Heritage walk

- Preventing - trucks and other commercial wagons from entering into core of the city.
- Efficient public transport system and encourage use of bicycles and non polluting vehicles within the core city.
- Development control rules for facades and buildings within city limit.
- Creation of a Heritage route linking the various heritage sites of the core city.
- Standardizing urban elements like – traffic islands, lights, street furniture, and pavements and fixing standard road level for the entire city.
- Establishment of “Madurai urban arts commission”.

## 8. MEENAKSHI TEMPLE SURROUNDS

The Meenakshi temple complex is one of the largest temples of South India, which is undoubtedly one of the oldest treasure troves of the country.

### 8.1 Temple profile

The walls of the temple enclose 830ft by 730ft of rectangular space with four massive gateways enclosing the shrines of Lord Shiva and Meenakshi Amman.

The 12 temple towers (Gopurams) and the holy temple tank known as Potramaraikulam (golden lotus pond) are some astounding features of the temple complex. The southern temple tower is the tallest measuring 170'6” with

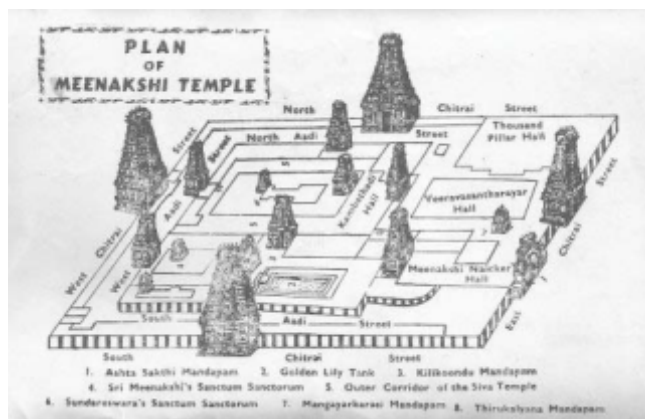


Fig. 8.1.1: Plan of Meenakshi Temple



Fig. 8.1.2: Aerial view of Meenakshi temple in 2002

1511 sudhai(idol) figures.

The north eastern corner of the temple houses the “Ayiramkaal mandapam” or the Hall of thousand pillar considered as an architectural masterpiece consists of 985 intricately carved stone pillars.

#### 8.1.1 Tempe Surrounds - Issues of concern:

- Once a celebrated space, was an eyesore for several decades. The lack of strict enforcement was the primary reason for the encroachment of the side pavement of Chithirai streets, by hawkers
- To any tourist or pilgrim, the imposing image created by the tall gopurams of the temple stands nullified because of the image created by the status of the nandhavanam – temple garden. The nandhavanam in the east and north have been converted as 2 wheeler parking.

#### 8.1.2 Tempe Surrounds - Identified potentials:

- Re-creation of a beautiful garden in the Nandavanam area can transform the image of the immediate surrounds of the temple.
- Basic visitor’s amenities like information kiosks, cloak rooms, slipper stands, and drinking water facilities can be achieved near the entry to the towers.

### 8.2 The Meenakshi park

A triangular open space lying at the junction of the east and north Chithirai Street, obtains its shape by the culmination of road route leading to the river Vaigai.

This fully fenced space was kept locked by the city authorities. This space consisted of a milk parlor and two pay and use toilets at the western end.



Fig. 8.2.1: Grills at exterior edge

### 8.2.1 Meenakshi Park - Issues of concern

- The provision of huge grills as barriers has led to the misuse of the exterior edge by the public and the interior by the antisocial elements.
- The enclosure of the park discourages the use of this shaded open space.

### 8.2.2 Meenakshi Park – Opportunities

- Its prominent location can transform itself into a green lung space for the core city dwellers, living in the most congested place of the city.
- A low level sunken amphitheatre shall permit the street performers and folk artisans to perform and entertain the pilgrims visiting the temple, also holding an opportunity to pave way for the dying folk culture.

### 8.3 The Chithirai streets

Outer streets running parallel to the Meenakshi temple walls is the Chithirai veedi(street) and it is through this street that any visitor has to enter the temple complex. The Chithirai streets are characterized by activities like textile shops, tourist amenity stores, banks, lodging and offices, etc.

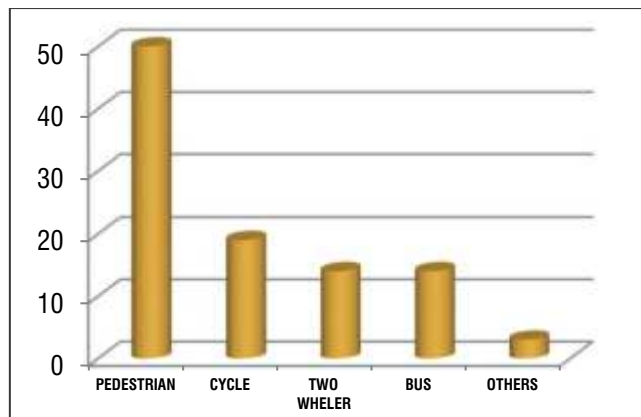


Fig. 8.3.1: % of vehicular movement in Chithirai Street

#### 8.3.1 The Chithirai streets - Issues of concern:

- Intrusion of the commercial shops and hawkers to display their products pushes the pedestrian movement into the road. Pedestrian movement is further hampered by the haphazard positioning of electrical lamp posts and transformers in the pavement.
- Lack of strong building bye laws had led this precinct of the ancient city to pose an incoherent look.
- Lesser space for pedestrian movement and maximized importance to vehicular movement with insufficient parking space had resulted in high pedestrian vehicular conflicts and congestion.
- Repeated laying of bitumen top road without removal of the previous layer, in due course of time had made the temple floor level sink below the road level, leading to the surface run off going into the temple and affecting the structure of the ancient monument.

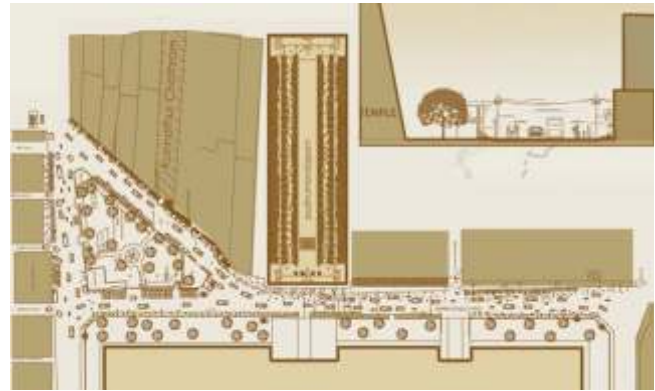


Fig. 8.3.1: East Chithirai Street – Road section - Earlier



Fig. 8.3.1: Views of East Chithirai Street - Earlier

- Several tourist information and advertisement hoardings put up at various places, including pavements had led to both physical obstruction and a visual pollution in the immediate surrounds of a world renowned heritage site.

#### 8.3.2 The Chithirai streets - Opportunities:

- This first street of the city, the image which any visitor to Madurai gets while entering in or out of the temple, has all possibilities of becoming the most imageable street.
- If provided with guided façade controls for all the shops and complimented with all tourist amenities and street furniture it can give a utilitarian and memorable experience to all the visitors.

### 9. DESIGN PROPOSAL

A comprehensive beautification design scheme for the Meenakshi temple surrounds was prepared and implemented in a phased manner.

#### Salient features of the proposal

- The existing bitumen road around the temple was dug up to 2 feet and 80mm thick paver blocks were laid without increasing the existing road levels in order to allow percolation of rainwater. With this implementation the road level around the temple which kept rising for sev-



Fig. 9.1: Proposed beautification design scheme - Plan



Fig. 9.2: Proposed beautification design scheme - Elevation



Fig. 9.3: Plan of the Proposed Meenakshi Park



Fig. 9.4: View of the Proposed Meenakshi Park

- eral decades came to an end.
- Based on our Principal Architect's vision and continuous struggle for more than 5 years, the Chithirai Streets that is the immediate surrounds of the Meenakshi temple was fully pedestrianised. Only battery cars and service vehicles are allowed to ply in the Chithirai streets.



Fig. 9.5: View of Chithirai Streets during beautification



Fig. 9.6: View of the paved chithirai streets



Fig. 9.6: Night life in pedestrianized chithirai streets

- Platforms were dressed with flamed granite stones, to match the Dravidian architecture with just 1500mm rise in level from paver blocks were provided.
- The entire space between the MMC road and the temple compound wall has been converted to landscape lawns. Earlier in an elaborate pilgrim waiting zones were created in this area but due to lack of funds, it was converted into green mounds.

## 10. CONCLUSION

- The Chithirai Street surrounding the temple was historically not designed to handle vehicles. Being a popular



Fig. 9.7: Aerial View of the Existing Pedestrianised Meenakshi Temple surrounds



Fig. 10.1: Chithirai street in 1915 (left) and 2001 (right)

tourist and pilgrimage spot worsened the situation by increasing pressure for parking.

- Pedestrianisation of the street has helped visitors and the citizens of the city to have a memorable and a user friendly experience this heritage marvel. It was brought back to its glory after several decades.

#### ACKNOWLEDGEMENTS

I would like to extend my sincere gratitude to all the government authorities like MMC, ASI, HR&CE, and other concerned organizations for their support.

I would also like to thank RR constructions, all the men and women labourers who worked in this project.



Fig. 10.2: Chithirai street in 2011

I thank the people of Madurai for their tremendous support in implementing this pedestrianization proposal.

Finally, I thank my family and staff of Karvin Design Studio for supporting me throughout this journey.

#### REFERENCES

- [1] Madurai Municipal Corporation detailed project report of Madurai's heritage corridor, Vol 1
- [2] ITDP – Pedestrianisation in India and across the globe

## Latvia completes a 93-km section of fence on Russian border

The fence was realized in order to address illegal migration. It is part of a bigger project which involves the construction of border infrastructure along the Latvian-Russian border. The project initiated in 2015 and is expected to be finished in 2020. The total length of the

wire fence along the borders of Latvia and Russia is expected to be approximately 284 km. The barrier is 2.7-meter-tall and topped with a barbed wire. It is constructed in strategic sections of the border, where the possibility of illegal passing is higher.

# Construction wastes used for manufacturing RA-bricks

**Armando Aguilar-Penagos<sup>1</sup>, Alberto López<sup>1</sup>, José Gómez-Soberón<sup>2</sup>, Nefalí Rojas-Valencia<sup>1\*</sup>**

<sup>1</sup>Universidad Nacional Autónoma de México, Instituto de Ingeniería, Coordinación de Ingeniería Ambiental, México

<sup>2</sup>Departamento de Tecnología de la Arquitectura, Universidad Politécnica de Cataluña, Barcelona, España

**Abstract:** In the Mexican republic, around 33.600 tons of construction wastes are generated every day, Mexico City contributing for around 7.000 tons/day, with fewer than 1.000 tons/day being sent to be recycled. This study relates to sustainable alternatives for recycling construction wastes, focusing on the manufacture of sustainable bricks using recycled aggregates (RA). The objective of this research was to manufacture RA-bricks of mixtures integrating clay excavation wastes, recycled binding aggregates from concrete having a particle size distribution of 3/8" and recycled mixed aggregates and binding wastes with a particle size distribution ranging from 1/4" to fines, wood cutting wastes and a liquid mixture of water and *Opuntia ficus-indica* (mucilage) extract as natural additive or stabilizer. A sustainable manufacturing process was used in which the clay material typically used in the traditional manufacturing of RA-bricks was replaced by excavation wastes of originally unknown composition obtained during the construction of two buildings, in order to investigate whether various excavation wastes having appropriate clay contents can be used as raw materials for manufacturing recycled aggregates bricks. Before using these wastes, preliminary particle size distribution, plasticity and hardness tests were performed in order to determine the appropriate residue dosages for manufacturing the bricks. The results showed that excavation wastes different from the clay soil usually used ensure the quality requested by the Mexican standard for non-structural adobe bricks. Currently, further studies are being conducted to promote their use in the manufacture of building elements.

## 1. INTRODUCTION

Brick is the masonry element most commonly used in the construction industry. Conventional bricks are produced from the firing of clay in oven at high temperatures, and the production of this material leads to the release of greenhouse gases, generally approximately 0.41 kilograms of CO<sub>2</sub> per unit manufactured [1] [2], leaving an important carbon footprint to the atmosphere.

In Mexico, 86.3% of homes are built with materials such as brick, partition, block, stone, quarry or cement [3], which provide quality inputs to the housing construction sector;

however, the production of these materials has an important impact on the environment, which has made the search for alternatives to solve the problem of pollution caused by the brick industry urgent.

Throughout the world, large amounts of construction and demolition waste are generated. In the European Union alone, 170 Mt are produced per year [4], while the United States produces 500 Mt/year [5]. In Mexico City the amount of construction and demolition waste generated has been increasing over the years due to the high demand for infrastructure, passing from 3,000 t/d in 2003 to 5,000 t/d in 2008 [6]. According to recent estimates [7], it currently reaches 12 Millions of t/year for the whole country, of which 1.3% is recycled in agreement with the guidelines of the Secretariat of the Environment and the Secretariat of Works and Services.

National standard NOM-161-SEMARNAT-2011 [8] establishes that construction waste must be classified as special management waste requiring appropriate actions for its reuse and recycling or, if applicable, correct disposal, while Mexico City standard, NADF-007-RNAT-2013 [6], classifies construction waste and proposes the use that should be given to these materials.

The growing generation of construction and demolition wastes has led to the idea of incorporating them in the manufacture of sustainable bricks, comparing, in terms of performance, their manufacture in an artisanal molding machine and in an industrial brick making machine. Moreover, the incorporation of a water-mucilage mixture is proposed for the homogeneous integration of the components, because previous research has shown that, when used as an additive in cement pastes, improved physical, mechanical and setting properties [9] are obtained. Water-mucilage mixtures have also permitted to achieve remarkable results in the restoration of historic buildings [10], the manufacture of paints (acting as waterproofing) for protection purposes [11], or the improvement of the erosion resistance of mud bricks [12].

As a contribution to the amelioration of the situation and based on the results from previous studies, the present research proposes an alternative for the use of construction waste, comparing artisanal and industrial manufacturing

processes.

## 2. METHODOLOGY

The study was divided in three stages: in the first stage, preliminary tests were carried out to determine the properties of the soil and the feasibility of using it as a binding material for the manufacture of the bricks; the second stage consisted of the manufacture of bricks in the artisanal molding machine and the conduction of mechanical tests, while in the third stage bricks were manufactured with an industrial brick making machine (mechanical tests were also performed).

The materials used for the manufacture of the bricks were as follows:

**Excavation waste:** The soil used was a mixture from San Francisco Coapa and Cuautlancingo, Puebla, which is a clay-sandy soil showing an adequate performance in the plasticity test and a high resistance in the hardness test.

**Construction Waste:** This material was provided by the company Recycled Concretes S.A. of C.V. located in the Iztapalapa delegation of Mexico City, and is classified into two large groups. The first group consists of cement-only construction waste, classified as type A according to NADF-007-RNAT-2013, coming from the crushing of concrete composite waste materials, with the selected granulometry ranging from 3/8" to 1/4". The second group called construction waste all in one, classified as type B by the same standard, coming from the crushing of bricks, blocks, ceramics, mortars, pavers, masonry and prefabricated composite materials with a selected granulometry of 1/4".

**Wood cutting residues:** These residues were provided by the composting plant of the National Autonomous University of Mexico, and were obtained from the cutting and pruning of trees, branches and shrubs from the University City. Prior to their use, the debris were "cleaned" using a 5 mm mesh rack.

**Liquid water-mucilage mixture:** Nopal units were obtained at the store called "Nopal-Verdura Collection Center" located in the Milpa Alta delegation in Mexico City. For the preparation of the mixture of water and cactus mucilage, the epidermis was removed from each unit, leaving only the mesophile. Squares of approximately 2 cm per side were cut and deposited in a container. The two-component combination was left to stand for three days. After the resting period, the liquid mixture was extracted with a strainer and then the pieces were placed in a cloth that served as a filter to extract the rest of the mixture by hand pressing.

**Mixture design:** The percentages of material used in the mixtures of the present research were obtained from the best of 11 mixtures, called 6, 7, 6-M, 7-M and shown in Table 1, distinguished by the construction waste used: only cementitious or construction waste all in one, in addition to water with nopal mucilage or water only as a liquid mixture for the integration of the components.

**Manufacturing process:** The equipment used in the manufacture of the bricks consists of a brick molding machine and a solar dryer, both manufactured in the carpentry of the Engineering Institute of the UNAM, and an industrial brick making machine.

Mixture	RC 1/4" SC	RC 1/4" TU	RC 3/8" SC	Water - Mucilage	Water	Excavation waste	Wood cutting waste
6	17	-	17	-	16	62	4
7	-	17	17	-	20		
6-M	17	-	17	19	-		
7-M	-	17	17	20	-		

RC: Construction waste; SC: Only cementitious; TU: All in one.

Table 1. Mixture Design

The second stage started with the manual preparation of the mixture. First, the dry materials were mixed with a shovel, then two-thirds of the water-nopal mucilage mixture were added with a graduated specimen and allowed to stand for a period of 10 minutes in order to hydrate the largest amount of dry material and were mixed to a uniform consistency at the end of the period, then the remainder of the liquid mixture was added and mixed to obtain the final consistency.

The mixture was then placed in the artisanal molding machine while manual compaction was carried out with the help of wood plates and applying a uniform force. Subsequently, final compaction was performed with the cap of the molding machine.

Finally the pieces were removed from the machine by applying a force to a lever. The manufacturing dimensions were chosen based on the standard NMX-C-441-ONNCCE-2013 [13]. Each piece had the following dimensions: length 26 cm, width 12 cm, height 5.5 cm.

Five pieces were made per type of mixture because it was the quantity needed to perform the subsequent tests. The manufactured parts were exposed outside for three days to achieve the greatest possible water loss and at the end of this period were introduced to the solar dryer to accelerate the drying process.

The brick manufacturing process of the third stage was similar to the process of the previous stage, the difference being the use of the industrial brick making machine instead of the artisanal molding machine, the manufacturing dimensions being as follows: length 30 cm. width 15 cm. height 5.5 cm.

## Essays

During the drying period, brick weight was monitored daily in order to determine the precise time when bricks stopped losing water and thus determine the time when the pieces were completely dry as well as the percentage of weight loss.

Resistance tests and water absorption tests were performed according to Mexican standards NMX-C-036-ONNCCE-2013 [14] and NMX-C-037-ONNCCE-2013 [15] respectively.

## 3. RESULTS

In order to analyze the behavior of the mixtures selected as optimal in both stages, the results of compressive strength and water absorption were compared and are

presented below:

**Determination of the drying period** The daily weight monitoring of each of the pieces of this phase was crucial to determine the end of the drying period which was considered as the time with no weight change from day to day or when weight change variation is close to zero. The results are shown in Figure 1 and in Figure 2 which correspond to the pieces of Mixture 6 and Mixture 7, respectively. Mixture 6 and Mixture 7 show the same drying period: 11 days after brick manufacturing. On day number 12, the weight is the same as, or very similar (about 1 g difference) to, the weight observed the previous day.

This behavior was also observed in the previous manufacturing stage. It was thus established that the solar drying optimum period is 11 days after manufacture, 3 days exposed outside and 8 days in the drying chamber.

The percentage of weight loss was also determined, and can be seen in Figure 1 and in Figure 2, which correspond to Mixtures 6 and 7, respectively. Water loss was about 20% for Mixture 6, while it was approximately 19% for Mixture 7. Eighty-five percent of water loss occurred during the first 5 days after the manufacture and only 15% during the remaining 6 days.

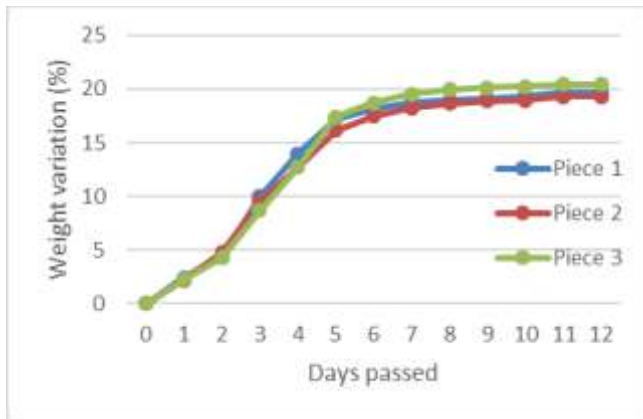


Figure 1. Percentage variation of daily weight - Mixture 6

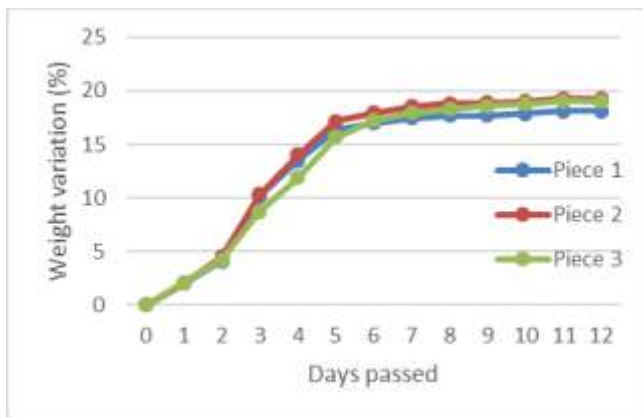


Figure 2. Percentage variation of daily weight - Mixture 7

**Solar dryer performance** The results obtained with the solar dryer are directly related to the environmental conditions. Although the tests were performed in winter (January), all the days on which measurements were made were sunny in phase III, while during phase II some days

were sunny and others were cloudy. Figure 3 shows the conditions presented by the solar dryer. The maximum indoor temperature was 92.4°C in phase III and 76°C in phase II, while the minimum temperature was 23.8 °C and 21.1° C, in phase III and phase II, respectively.

Figure 4 shows the solar radiation captured by the dryer with phase III having a maximum reception of 1132.2 W/m<sup>2</sup> compared to 733.4 W/m<sup>2</sup> for phase II. The minimum reception was 34.0 W/m<sup>2</sup> and 43.3 W/m<sup>2</sup> for phase III and phase II, respectively.

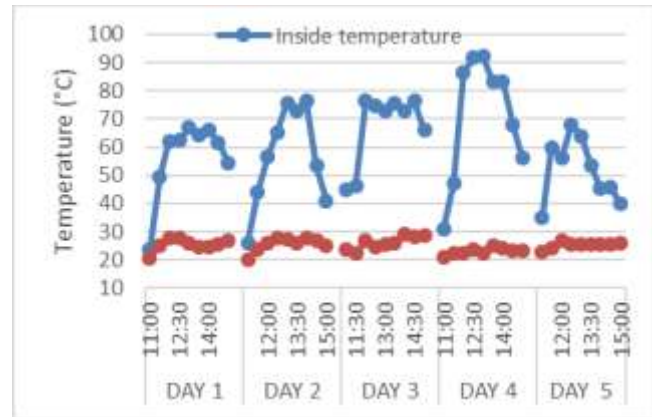


Figure 3. Condition of temperature with respect to the drying period.

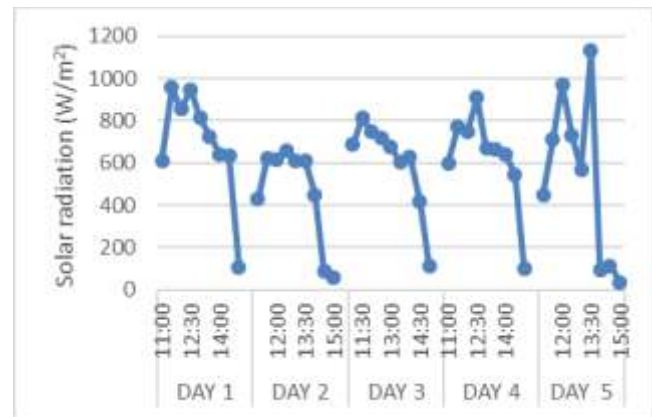


Figure 4. Solar radiation captured by the dryer during the established period.

**Compressive strength** Compressive strength results obtained with both stages are shown in Figure 5, with a resistance reduction of approximately 19% for Mixture 6 and 29% for Mixture 7 in stage III.

Although the results of stage III remained above the minimum limits established by the regulations, the behavior was not as expected, since the use of an industrial brick making machine was assumed to lead to an improved compaction of the mixture and thus to a compressive strength increase, which did not occur. This unexpected behavior is attributed to the use of aggregates having a 3/8 "granulometry, which did not allow proper compaction, so that the pieces had holes in their matrix leading to a poor performance.

**Initial Maximum Water Absorption** Figure 6 shows the comparison of initial maximum water absorption results. The values obtained with Mixtures 6 and 7 in Stage III far



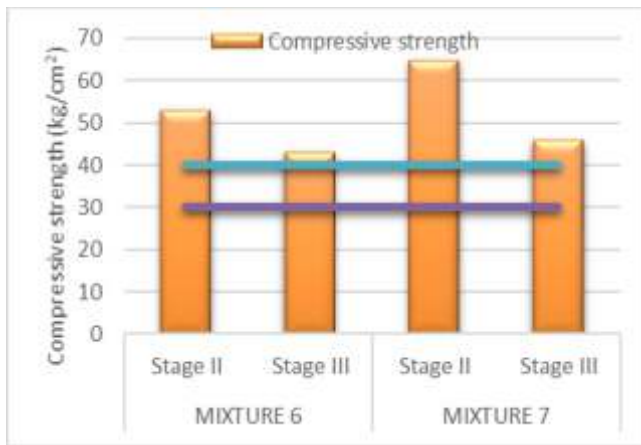


Figure 5. Comparison of compressive strength between both manufacturing stages.

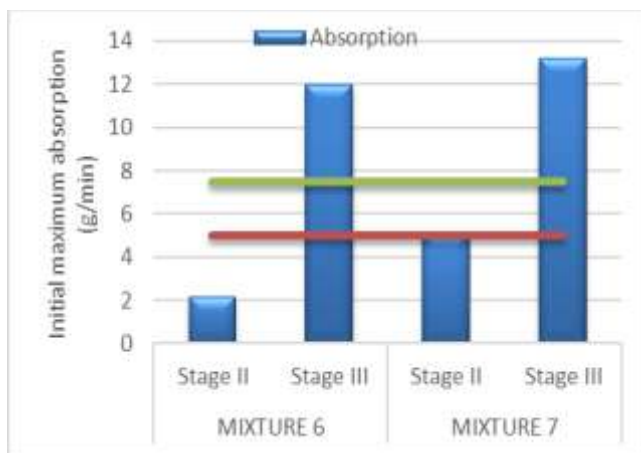


Figure 7. Comparison of initial maximum water absorption between the two manufacturing stages.

exceeded (81% and 62% in the case of Mixture 6 and Mixture 7, respectively) the values obtained in Stage II, which exceed the maximum parameters permissible by Mexican regulations for interior and exterior walls.

The objective of using a brick making machine to manufacture blocks was to improve mechanical properties (compressive strength, water absorption); however, the response was adverse. This behavior is accompanied by the analysis of the compressive strength, the holes in the matrix of the blocks caused by the construction residues with 3/8 granulometry provoked a greater permeability, generating a sharp increase in water absorption values.

#### 4. CONCLUSION

The constructive process proposed was efficient for the manufacture of bricks, using both an artisanal as well as an industrial method.

The drying period in the solar dryer is 11 days in the case of artisanal and industrial bricks and with both mixtures.

Taking into account all the conditions tested it can be said that the maximum temperature recorded was 92.4 °C and the minimum temperature was 21.1 °C. The maximum solar radiation captured by the dryer was 1132.2 W/m<sup>2</sup> and the minimum 34.0 W/m<sup>2</sup>. In clearer and sunnier areas,

temperature and radiation increase significantly.

In all cases, weight stabilized after six days.

Despite a reduction in compressive strength and an increase in water absorption, the bricks manufactured in this research are a sustainable alternative for the use of construction waste since they comply with the quality parameters established in the Mexican norm.

The use of nopal mucilage for the integration of the liquid mixture for brick manufacturing represents an alternative because it makes use of the large quantity of nopal that is disposed of as waste, and gives a new application to that organic material that helps improve the mechanical properties of bricks.

The final behavior of the bricks manufactured in this research shows that they can be used without major difficulties in the construction sector.

The cost of production of this ecological block makes it an economical option for the construction sector by providing a quality material that meets the parameters required by the current standards.

#### 5. RECOMMENDATIONS

It is important to consider that when the excavation materials come from different sites, corresponding tests must be carried out to know their properties and make an appropriate mixture design. It should be noted that not all excavation materials can be used for the manufacture of blocks.

There is a contradiction in the sense of not using aggregates with granulometry of 3/8" for the manufacture of bricks and using only granulometry of 1/4", because in Stage I mixtures containing this aggregate size were selected as optimum, but this recommendation was proposed because the company marketing the machine operates with particle sizes (excavation material) smaller than 3/8" for the production of its blocks, and this could be the cause of the decrease in the compressive strength observed between the artisanal and the industrial bricks.

It is also recommended to change the dimensions of the blocks designed in Stage II, since with a greater proportionality ratio, blocks can have better physical and mechanical properties.

For the manufacture of bricks carried out on the machine used in Stage III, it is recommended to design mixtures only with construction and demolition waste of 1/4" for greater integration of the components in the pressing chamber.

The recommendation to change the size of the blocks in Stage II is also for constructive reasons, since, if a block of larger dimensions is manufactured, fewer pieces will be used for the configuration of constructive elements, leading to a faster advance in the work program, and a lower cost.

The creation of a mini processing plant is recommended to produce blocks with a higher efficiency.

#### ACKNOWLEDGEMENTS

The authors express thanks to II-UNAM and to the scholarships program for Master Degree studies by CONACYT.

## REFERENCES

- [1] Reddy BW, Jagadish KS. Embodied energy of common and alternative building materials and technologies. *Energy Build* 2003; 35:129–37.
- [2] Lippiatt BC. BEES 4.0 – Building for environmental and economic sustainability. Technical manual and user guide. NISTIR 7423; 2007.
- [3] INEGI. (2010). Banco de información INEGI. Obtenido de <http://www.inegi.org.mx/sistemas/biinegi/?ind=3114003001> (in Spanish).
- [4] R. V. Silva, J. De Brito, and R. K. Dhir, "Properties and composition of recycled aggregates from construction and demolition waste suitable for concrete production," *Constr. Build. Mater.* Vol. 65, pp. 201–217, 2014.
- [5] F. J. Colomer, J. Esteban, and A. Gallardo, "Application of inert wastes in the construction, operation and closure of landfills: Calculation tool," *Waste Manag.* Vol. 59, pp. 276–285, 2017.
- [6] NADF-007-RNAT-2013. Norma ambiental para el Distrito Federal. Clasificación y especificaciones de manejo para residuos de la construcción y demolición en el Distrito Federal. (in Spanish).
- [7] Granell, E. (2014). Experiencia empresarial de los RCD en México. México, D. F.: Concretos Reciclados. (in Spanish).
- [8] NOM-161-SEMARNAT-2011; Que establece los criterios para clasificar a los Residuos de Manejo Especial y determinar cuáles están sujetos a Plan de Manejo; el listado de los mismos, el procedimiento para la inclusión o exclusión a dicho listado; así como los elementos y procedimientos para la formulación de los planes de manejo. (in Spanish).
- [9] León-Martínez F, Cano-Barrita P, Lagunez-Rivera L and Medina-Torres L (2014) Study of nopal mucilage and marine brown algae extract as viscosity-enhancing admixtures for cement based materials. *Construction and Building Materials* 53: 190–202.
- [10] Ventola L, Vendrell M, Giraldez P and Merino L (2011) Traditional organic additives improve lime mortars: new old materials for restoration and building natural stone fabrics. *Construction and Building Materials* 25(8): 3313–3318.
- [11] Cárdenas, A., Arguelles, W., & Goycoolea, F. (2002). On the possible role of *Opuntia ficus-indica* Mucilage in Lime Mortar Performance in the Protection of Historical Buildings. Hermosillo: Centro de Investigación en Alimentación y Desarrollo. Obtenido de [http://jpacd.org/downloads/Vol3/RAC\\_4.pdf](http://jpacd.org/downloads/Vol3/RAC_4.pdf) (in Spanish).
- [12] Martínez-Camacho F, Vázquez-Negrete J, Lima E, Lara V and Bosch P (2008) Texture of nopal treated adobe: restoring Nuestra Señora del Pilar mission. *Journal of Archaeological Science* 35(5): 1125–1133.
- [13] NMX-C-441-ONNCCE-2013. Norma Mexicana - Industria de la construcción – Bloques, tabiques o ladrillos y tabicones para uso no estructural –Especificaciones. (in Spanish).
- [14] NMX-C-036-ONNCCE-2012. Norma Mexicana - Industria de la construcción – Bloques, tabiques o ladrillos, tabicones y adoquines- Resistencia a la compresión – Método de prueba. (in Spanish).
- [15] NMX-C-037-ONNCCE-2013. Norma Mexicana - Industria de la construcción-Mampostería – Determinación de la absorción total y la absorción inicial de agua en bloques, tabiques o ladrillos y tabicones – Método de ensayo. (in Spanish).

## Geopier's GP3<sup>®</sup> ground improvement system to support heavily-loaded grain storage bin

**A**t Madison Farmers in South Dakota, a new grain storage bin has been constructed adjacent to two existing grain storage bins. The Geopier GP3<sup>®</sup> ground improvement system provided significant cost savings and schedule advantages while keeping the existing grain bins operational.

The new bin has a diameter of 135 feet and an eave height of 91 feet, with a capacity of 1.1 million bushels. The bin is supported by a ring footing with an 8-foot tall stem wall with an above-ground reclaim tunnel. Subsurface conditions consist of up to 8.5 feet of very stiff lean clay

and medium dense clayey sand FILL underlain by medium stiff to stiff lean clay (alluvium) overlying medium dense to dense sand (alluvium) followed by stiff to very stiff sandy lean clay (glacial till) to the maximum explored depth.

The suggestion of the project's geotechnical engineer was to over-excavate and refill with off-site granular structural fill, but due to site challenges/ restrictions, this would have required temporary shoring to allow the existing bins to remain in use.

# Sustainable Concrete Solutions for Buildings in the UK

**Costas Georgopoulos<sup>1\*</sup>, Andrew Minson<sup>2</sup>**

<sup>1\*</sup> Professor in Structures & Head of the Department of Civil Engineering, Kingston University, UK

<sup>2</sup> Executive Director, The Concrete Centre, Mineral Products Association, UK

**Abstract:** The UK concrete industry has a vision to be recognised as a world leader in sustainable concrete production. The annual concrete industry sustainability report sets targets and measures data over various sustainability criteria and new 2020 commitments include continuous improvement of Sustainability Production Performance, Life Cycle Assessment Data and a Material and Resource Efficiency Programme to inform best practice.

Sustainable material specification aims to specify concrete with low environmental impact whilst ensuring other inherent performance credentials such as durability are optimised. Good practice includes specifying low carbon cement blends, considering recycled or secondary aggregates, not over-specifying concrete strength, maximising cementitious additions in foundations or where striking times are not critical and, specifying responsibly sourced concrete and reinforcement.

Efficient structural design aims to optimise material use and reduce waste e.g. post-tensioned slabs that can provide thinner longer spans with fewer columns and lighter foundations. Nevertheless truly sustainable buildings require a holistic approach whereby whole life impacts including concrete's thermal mass –balanced impacts of construction stage with operational stage –are minimised.

This paper presents latest developments in the design and construction of sustainable concrete framed buildings with relevant case studies and looks at the future of sustainable concrete in the UK.

## 1. INTRODUCTION

In support of its vision to be recognised as a world leader in sustainable concrete production, the UK concrete industry has set strategic objectives and commitments with the scope to monitor and deliver the best sustainable construction with concrete in a socially, environmentally and economically responsible manner.

The annual concrete industry sustainability report sets targets and measures data over various sustainability criteria. For example CO<sub>2</sub> emissions per tonne of cement have decreased by 22% between 1998 and 2013 and, the proportion of fuel comprising waste material in 2013 was 44% of the thermal input to the kiln (up from just 6% in 1998).

New 2020 commitments include continuous improvement of Sustainability Production Performance, Life Cycle Assessment Data and a Material and Resource Efficiency Programme to inform best practice [1].

Sustainable construction and operation of the built environment using concrete can only be achieved if the right decisions are taken at the design stage. The role of the Structural Engineer in the decision making process offers limited but distinct opportunities to contribute positively or negatively to sustainable development. Although true integration across several disciplines is essential for maximum impact, the Structural Engineer's contribution is mainly focused on sustainable material specification and efficient structural design [2].

Sustainable material specification aims to specify concrete with low environmental impact whilst ensuring other inherent performance credentials such as durability are optimised. Good practice includes specifying low carbon cement blends, considering recycled or secondary aggregates if available locally, not over-specifying concrete strength, considering conformity to 56-day rather than the conventional 28-day strength, maximising cementitious additions in foundations or where striking times are not critical and, specifying responsibly sourced concrete and reinforcement [3].

Efficient structural design aims to optimise material use and reduce waste e.g. post-tensioned slabs that can provide thinner longer spans with fewer columns and lighter foundations. Nevertheless truly sustainable buildings require a holistic approach whereby whole life impacts –balanced impacts of construction stage with operational stage including demolition –are minimised achieving material resource efficiency. For example, exposed fair-faced concrete walls offer both a lean structural solution as well as efficient energy performance via thermal mass. The undisputable durability, robustness and long-life properties of concrete also facilitate the re-use of existing concrete structures, therefore reducing future demolition waste [4].

## 2. CONCRETE INDUSTRY SUSTAINABILITY PERFORMANCE REPORT

Based on data collected for concrete production, the

annual sustainability report provides an update on progress made for a range of performance indicators against 2020 targets. A summary for the period 2008 to 2015 is outlined below with 2020 targets in parenthesis:

- **Environmental Management (95%):** the percentage of the total concrete production and constituent materials sites that are independently certified to ISO14001. Starting from 72.3% in 2008 it has continued to increase reaching 93% in 2015.
- **Quality and Performance (95%):** the percentage of the total concrete production and constituent materials sites that are independently certified to ISO9001. Starting from 84.2% in 2008 it has continued to increase reaching 93.9% in 2015.
- **Responsible Sourcing (95%):** the percentage of concrete and constituent materials production that is certified by a third party to BES6001. Starting from 81% in 2009 it has continued to increase reaching 89% in 2015.
- **Resource Efficiency (35%):** the percentage additional cementitious materials (e.g. by-products such as GGBS and fly ash) as a proportion of the total cementitious materials. Starting from 30% in 2008 it has struggled to increase with 29% in 2015.

This indicator is strongly influenced by the types of concrete required by the construction industry.

Another indicator of Resource Efficiency is the use of Recycled / secondary Aggregates as a proportion of total aggregates in concrete. This is affected by transportation emissions and the implications of mix design. No target has been set as increasing recycled content is not always indicative of sustainable performance. In 2015, 6.4% of aggregates used in concrete were from recycled or secondary sources.

A final indicator under Resource efficiency is the use of Recycled Steel Reinforcement i.e. the percentage of recycled scrap as a proportion of total constituent raw materials used. This always depends on availability and it has been fluctuating from 97% in 2009 to 93% in 2015.

- **CO<sub>2</sub> Emissions – Production (-30% from 1990 i.e. to 72.2kg CO<sub>2</sub> / tonne of concrete):** For the two types of mixes in 2015, 'rolling mix' value in kg CO<sub>2</sub> / tonne of concrete was 80.3 from 87.5 in 1990 and the 'standardised mix' was 73.8 from 87.5 in 1990 i.e. overall reductions of 9% and 19% respectively.
- **CO<sub>2</sub> Emissions – Transport (kg CO<sub>2</sub> / tonne of concrete –target under review):** CO<sub>2</sub> emissions of total delivery transport through the industry supply chain in kg CO<sub>2</sub> / tonne. The value for 2015 was 8.4 fluctuating from 7.2 in 2009.
- **Waste Minimization (-90% from 2008):** percentage of waste to landfill as a proportion of production output. Starting from 4.4% in 2009 it has continued to decrease reaching 1.2% in 2015 i.e. an impressive 90% reduction reaching the 2020 target. The landfill tax has played an

important role but also, the changing industry culture towards waste.

- **Replacement of Fossil Fuels (50%):** the proportion of energy derived from the waste stream for use as a fuel source, as a percentage of total energy use. Starting from 17.4% in 2008 it has continued to increase reaching 32.5% in 2015.
- **Biodiversity (100%):** percentage of relevant production sites that have site specific action plans. Starting from 94.3% in 2008 it has continued to increase reaching 99.4% in 2015.
- **Water (target to be set in 2018):** mains water consumption as a proportion of water in production output. Starting from 86% in 2008 it has continued to reduce reaching 78.3% in 2015.
- **Health and Safety (reduce lost time injuries to 1.19 by 2019 with an aim for zero harm):** number of lost time injuries for direct employee per 1,000,000 hours worked. Starting from 6.5 in 2010 it has continued to decrease but with a sudden increase to 4.3 in 2015 from 3.4 in 2014. Incidents are reviewed and key learning points are shared across the sector to improve performance.
- **Employment and Skills (100%):** percentage of employees covered by certified training and evaluation processes. Starting from 87.3% in 2009 it has continued to increase reaching 95.8% in 2015.
- **Emissions (excluding CO<sub>2</sub>) (zero):** number of convictions per annum for air and water emissions. Starting from 6 in 2008 it has continued to reduce reaching zero in both 2014 and 2015.
- **Local Community (100%):** percentage of relevant sites that have community liaison activities. Starting from 85.9% in 2008 it has continued to increase reaching 100% in 2015. Community liaison activities include group, council and public meetings, community newsletters, social, recreational and educational initiatives.

### 3. SPECIFYING SUSTAINABLE CONCRETE

For a long time, the main challenge of sustainability has been to clearly identify and appropriately quantify the impacts of many factors that affect the sustainability performance of buildings and infrastructure over their whole-life i.e. 'cradle to grave' and eventual demolition with potential recycle. It is now encouraging that new European standards, EN 15804 for products and EN 15978 for whole buildings, provide the framework and methodology for measuring whole-life impacts. In anticipation of these standards the concrete industry in the UK has been pro-active for a number of years and has already launched generic environmental product declarations (EPDs) in accordance with EN 15804 for a range of concrete products. EPDs help concrete specifiers.

Current standards for specifying concrete in the UK i.e. BS EN 206 and BS 8500 do not include any provisions for specifying sustainable concrete. The following key

guidelines are provided by The Concrete Centre to engineers and other specifiers in the UK to enable them to specify sustainable concrete whilst ensuring that its performance benefits are optimised.

- Specify BES 6001 responsibly sourced concrete and reinforcement. The industry is committed to offer the highest level of responsible sourcing.
- Aggregates are inherently a low carbon product although they are the major component of concrete. When specifying recycled and secondary aggregates, availability and cost (with aggregates levy and landfill tax built-in) must balance primary aggregate resource depletion (no problem in the UK although not acknowledged in BREEAM material assessments –EPDs can be used to change that), transportation CO<sub>2</sub> emissions (if delivery distance is more than an extra 15km carbon footprint of recycled aggregates is greater than primary aggregates) and implications on mix design (e.g. potential increase in water demand with a need for more cement for the same strength). As aggregate size has a significant impact on cement content, do not specify aggregate sizes below 10mm unless necessary. Discussions with client and contractor are recommended.
- Cement represents the majority of the embodied CO<sub>2</sub> (ECO<sub>2</sub>) of concrete. The UK cement industry has made significant progress in reducing the ECO<sub>2</sub> of cement by using waste-derived fuel and incorporating additional cementitious materials [5]. Its roadmap has two scenarios showing what is possible with and without carbon capture and storage / use scenarios 1 and 2 respectively (see Fig 1). At the same time, a number of by-products from other industries, defined as 'cementitious additions', can be blended with Portland cement to reduce ECO<sub>2</sub> but also to improve performance such as GGBS (50%), fly ash (25%), silica fume (10%) and limestone fines (6-10%) with figures in parentheses showing the most common proportions by mass of total cementitious content used in the UK. Notwithstanding the effect of additions to surface colour that must be taken into account, early strength development can be an issue with concrete mixes containing more than 50% GGBS not achieving sufficient strength after one day to allow removal of vertical formwork, particularly at lower temperatures, and therefore adversely affecting the construction programme. Specialist Contractors in the UK are able to erect in-situ concrete structures and indeed high-rise concrete framed buildings to programme with low ECO<sub>2</sub> concrete mixes using established as well as innovative methods and testing techniques. The advice is 'do not over-specify concrete strength and consider the possibility of strength conformity at 56 rather than 28 days (see Fig. 2).
- Allow the use of recovered or combined water for both

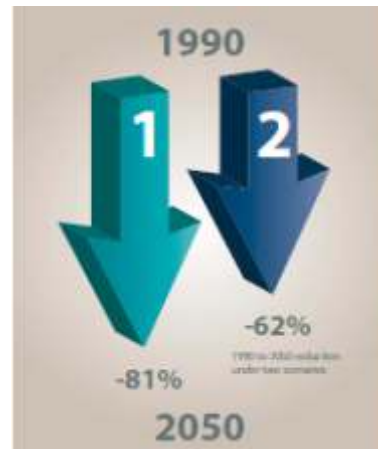


Fig. 1: MPA scenarios for greenhouse gas reduction for cement production from 1990 to 2020 with and without carbon capture and storage



Fig. 2: The Shard is the tallest building in the UK and currently in Europe. The C35/45 concrete contains a cement blend using 70% GGBS to limit early heat generation. This high level of additional cementitious material has the potential disadvantage of low early strength. This was overcome by developing the concrete so that it would achieve sufficient strength to meet initial structural requirements within 14 days with the full strength being achieved at 56 days.

un-reinforced and reinforced concrete and, consider its influence on air-entrained concrete or concrete exposed to aggressive environments or the visual impact on exposed concrete.

- Permit the use of admixtures that can significantly improve the physical properties of concrete in the fresh and hardened state but also, enhance the sustainability

credentials of concrete and reduce its  $\text{ECO}_2$  (for example the use of a water-reducing admixture enables a given water cement ratio or strength to be achieved with lower cement content).

- Reinforcement adds approx. 15kg  $\text{ECO}_2$  / tonne of concrete (re C28/35 unreinforced concrete has 95kg  $\text{ECO}_2$  rising to 110 if reinforced). It is however important in sustainable 'lean' design to minimise material use including the amount of reinforcement.

#### 4. MATERIAL RESOURCE EFFICIENCY

Notwithstanding sector initiatives to improve material efficiency such as the Resource Efficiency Action Plans that assist the supply chain in managing material efficiency from cradle to grave incl. demolition - see other initiatives in the Concrete Industry Sustainability Report section - concrete is made of materials that can be locally and sustainably sourced throughout the UK, as follows:

- **Aggregates:** The UK has an abundance of local, primary naturally-occurring aggregates which, with permissions provided, could last thousands of years. Mineral extraction is tightly regulated and quarries are restored delivering biodiversity. The average road delivery distance for aggregates is 51.5km.
- **Cementitious Materials:** Every cement plant in the UK is replacing fossil fuels by other waste alternative fuels such as solvents, tyres, meat and bone meal, sewage sludge, un-recyclable paper and plastics. In parallel, additional cementitious materials such as GGBS and fly ash have been used for many years.
- **Steel Reinforcement:** UK produced reinforcement is 100% recycled steel that is produced using Electric Arc Furnace technique which uses significantly less energy.

Concrete is manufactured in a spectrum of resource efficient solutions such as the following:

- **Precast Concrete:** Factory-based formwork that can be used many times; products made to order and 'just-in-time' delivery and installation that minimise waste; high quality finishes unaffected by the weather.
- **Blockwork:** Using very high levels of recycled materials including furnace bottom ash aggregates, industrial slags and returned concrete products; blocks are typically a very low waste product.
- **Ready-mixed Concrete:** 'Just-in-time' delivery with average delivery distance for ready-mixed concrete being 11km; the relatively small amount of unused concrete is then recovered by batching plants.
- **Formwork and Falsework:** Facing plywood or metal forms made from recycled steel achieve good quality finish are reused many times. Permanent formwork systems such as Insulated Concrete Formwork, twin wall construction and lattice girder slabs are also used in the UK.

Design of framed structures offers a wide range of

resource efficient solutions in precast, in-situ or hybrid concrete. 'Lean' design ensures that material is used only where is needed by considering the following:

- Select solutions to optimise different span and span ratio arrangements
- Choosing large spans may not be the most material efficient solution
- Use structural continuity for connections can reduce structural depths
- Achieve a balance between element size and amount of reinforcement
- Minimise floor depths for less material, cladding, cores, walls and foundations. But watch acoustic properties of thin slabs that may require suspended ceilings
- Select resource efficient shapes and forms such as thin shell structures.
- Consider using fin columns as part of building and room enclosures
- Reduce waste by regularity i.e. avoid off-cuts and bespoke elements
- Obtain credits with BREEAM by taking measures to optimise material efficiency.

Concrete's inherent performance in durability, fire resistance and acoustic separation is supplemented by thermal mass that offers lifecycle cost and environmental impact savings. A case study is shown in Fig 3 below:



Fig. 3: Burntwood School, London. Precast cladding panels were pre-glazed with insulation added in the factory, significantly reducing wastage; Exposed concrete soffits throughout to provide thermal mass; Concrete slabs, stairs, classrooms, etc. with no finishes provide attractive no-waste no-maintenance hard-wearing surfaces appropriate for a tough school environment.

To reduce cost and landfill tax, reducing waste on site is a key consideration for UK Contractors who, through Site Waste Management Plans, demonstrate ways in which waste has been avoided or minimised through design or procurement decisions and site practice. Some considerations are avoiding over-ordering, careful handling and storage on site, good workmanship and quality control, minimising changes in specification or construction programme and

using off-site solutions where feasible.

The cost of a structural frame including its foundations, cores and structural elements represents a relatively small percentage of the total cost of a multi-storey building in comparison with the cost of finishes, services, cladding, etc. Therefore designing the structural frame to last longer than the conventional 60-year life span makes sense being cost effective and allowing its reuse in the future. This is achieved best by choosing concrete frames and simply increasing the cement content or the cover to reinforcement and, unreinforced masonry remains functional for well over 100 years. In addition, concrete and masonry require little or no maintenance to prevent material degradation.

Concrete and masonry provide inherently resilient and cost-effective solutions to climate change including reducing the risk and impact of flooding and overheating. Sustainable design should include thinking about future performance, see case study in Fig. 4 below:



Fig. 4: Ash Court, Girton College, Cambridge. A residential wing providing 50 en-suite bedrooms, gym accommodation and an indoor swimming pool; Resilience to climate change has been addressed by installing plastic pipework in the exposed concrete soffits, allowing active surface cooling to be used in the future. This added little to project costs.

Concrete structures are durable and robust and cost effectively adapted for reuse - extending the life of a building for more than 60 years, see case study in Fig. 5 below:

Current practice in the UK is that the majority of concrete demolished on site, is used on site. The common cost-effective use of concrete demolition waste is as rubble for hard core, fill or landscaping, especially if it contains other materials as brick. When concrete is crushed during demolition the carbonation process occurs and continues during the concrete's secondary life if used in groundworks. A significant amount of CO<sub>2</sub> emissions is reabsorbed through carbonation during life and particularly end of life and, this is a very important factor when calculating whole-life CO<sub>2</sub>.



Fig. 5: Elizabeth II Court, Hampshire Council Offices, Winchester. The existing over 50yrs old concrete frame was retained, significantly reducing demolition waste, and the existing concrete cladding was removed, crushed and reused as aggregate in other materials. Previously hidden concrete soffits were exposed and painted, enabling the concrete, due to its thermal mass, to provide comfort and energy performance through passive design measures.

## 5. CONCLUSION

It is evident from Section 2 of this paper that the vast majority of indicators used to monitor the sustainability performance of concrete production in the UK have continued to improve and would most certainly reach the ambitious targets set by the concrete industry in 2008. Despite the uncertainty of Brexit, the concrete industry is committed to its strategy for sustainable concrete construction and will continue to monitor and improve its performance.

With regard to specifying sustainable concrete in Section 3, there are plenty of case studies to demonstrate that, in the UK, specifiers increasingly recognise and utilise the full advantage of the sustainability credentials of concrete including durability, robustness, fire resistance, thermal mass, acoustic performance and flood resilience. Accepted good practice for designers is not to simply follow a tick box mentality in using assessment tools that are general and not applicable for every project but to take a holistic and whole-life view of sustainability.

Whole-life approach to material resource efficiency is also recommended in Section 4. Using concrete and masonry in the UK offers many opportunities to do more for less with resource efficient manufacture and established design practice for material efficiency in use, longevity, reuse and material recovery after demolition.

## 6. FUTURE

Three examples of developments in the future of sustainable concrete solutions in the UK relate to a constituent, design information and a new means of utilising concrete's thermal mass:

**Cements** - increasing use of limestone powder: Limestone powder is already used in combination with Portland cement clinker to make cement –known as Portland limestone cement (PLC) –which usually contains about 15%

limestone powder. In the UK, PLC is designed to meet performance criteria for most building applications and is permitted by application standards. While PLC is available in bulk, the majority is currently supplied in bags. Possible solutions for optimising the use of limestone powder in the production of cement include either manufacturing higher strength PLC or incorporating limestone powder in three-component CEM I-fly ash-limestone or CEM I-GGBS-limestone composite cements. Such practices are now commonplace in many European countries, and such cements are covered by the European cement standard EN 197-1. However, the use of three-component, limestone containing cements is still not permitted by UK application standards. A current MPA project is to provide a case for standardisation so that new three-component, limestone-containing cements can be included in the UK concrete standard, BS 8500. This would enable specifiers to improve resource efficiency without compromising performance. [6]

**Environmental Product Declarations (EPD) and Building Information Modelling (BIM):** With data on maintenance, lifespans and energy performance of different components, the whole-life impact of a built asset can be planned for when using a comprehensive BIM for a project. Information taken from environmental product declarations (EPDs) linked to BIM objects will allow architects and designers to model the embodied impacts of their material and design choices. If the model is kept up to date, it can provide a good starting point for any alterations or extensions to the asset. At the end of the building's life, the model can inform safe demolition and also the specifications for recycling. The thinking can be shifted from capital to whole-life cost. [6]

**Concrete for Smart Energy Storage:** The shift to renewable power, which now accounts for 14% of the UK supply, results in the challenge of an increasing imbalance between supply and demand. Concrete and masonry have the ability to store and release heat—their thermal mass—which can be used as the basis of a demand-side-response electric heating

system. This involves using the floors and walls in medium and heavyweight buildings as a form of storage heater, linked to an intelligent control system that takes advantage of electricity when demand and price are low. At other times, the heating is switched off as much as possible and comfort is maintained by the slow release of stored heat. This in itself is not particularly ground breaking, but the roll-out of smart meters in the UK that can respond directly to real-time energy pricing and link to heating controls will result on an opportunity for designers and building owners. [6]

## REFERENCES

- [1] MPA-The Concrete Centre (2017) Concrete Industry Sustainability Performance Report, 9th report: 2015 performance data, MPA-The Concrete Centre on behalf of the Sustainable Concrete Forum, UK.
- [2] Georgopoulos C., Minson A. (2014), Sustainable Concrete Solutions, book for students, academics and practitioners, Wiley Blackwell, Publishers, UK. ISBN: 978-1-119-96864-1, 256pp.
- [3] MPA-The Concrete Centre (2017) Specifying Sustainable Concrete, Understanding the role of constituent materials, MPA-The Concrete Centre, UK, ISBN 978-1-908257-01-7, 23pp.
- [4] MPA-The Concrete Centre (2016) Material Efficiency, Design guidance for doing more with less, using concrete and masonry, concrete, MPA-The Concrete Centre, UK, ISBN 978-1-908257-15-4, 19pp.
- [5] MPA-Cement (2017) Sustainable Development Report 2016, cement in the circular economy, MPA-Cement, UK, 14pp.
- [6] MPA-The Concrete Centre (2017), New Ideas and Good Ideas that Never Get Old, MPA-The Concrete Centre, UK, 20pp.

## 'Deep learning' casts wide net for novel 2D materials

Researchers at Rice University's Brown School of Engineering say they can find out fast by feeding basic details of their structures to "deep learning" agents that have the power to map the materials' properties. Better yet, the agents can quickly model materials scientists are thinking about making to facilitate the "bottom-up" design of 2D materials.

Rouzbeh Shahsavari, an assistant professor of civil and environmental engineering, and Rice graduate student Prabhas Hundi explored the capabilities of neural

networks and multilayer perceptrons that take minimal data from the simulated structures of 2D materials and make "reasonably accurate" predictions of their physical characteristics, like strength, even after they're damaged by radiation and high temperatures.

Once trained, Shahsavari said, these agents could be adapted to analyze new 2D materials with as little as 10 percent of their structural data. That would return an analysis of the material's strengths with about 95 percent accuracy, he said.



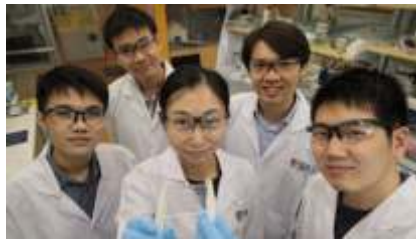
## Water-resistant electronic skin with self-healing abilities created

A team of scientists from the National University of Singapore (NUS) have taken inspiration from underwater invertebrates like jellyfish to create an electronic skin with similar functionality.

Just like a jellyfish, the electronic skin is transparent, stretchable, touch-sensitive, and self-healing in aquatic environments, and could be used in everything from water-resistant touchscreens to aquatic soft robots.

Assistant Professor Benjamin Tee and his team from the Department of Materials Science and Engineering at the NUS Faculty of Engineering developed the material, along with collaborators from Tsinghua University and the University of California Riverside.

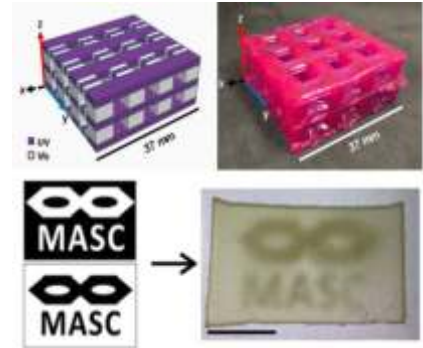
The team of eight researchers spend just over a year developing the material, and its invention was first reported in the journal *Nature Electronics* on 15 February 2019.



Asst Prof Tee has been working on electronic skins for many years and was part of the team that developed the first ever self-healing electronic skin sensors in 2012.

His experience in this research area led him to identify key obstacles that self-healing electronic skins have yet to overcome. "One of the challenges with many self-healing materials today is that they are not transparent and they do not work efficiently when wet," he said. "These drawbacks make them less useful for electronic applications such as touchscreens which often need to be used in wet weather conditions."

## Light provides control for 3D printing with multiple materials



3D printing has revolutionized the fields of healthcare, biomedical engineering, manufacturing and art design.

Successful applications have come despite the fact that most 3D printing techniques can only produce parts made of one material at a time. More complex applications could be developed if 3D printers could use different materials and create multi-material parts.

New research uses different wavelengths of light to achieve this complexity. Scientists at the University of Wisconsin-Madison developed a novel 3D printer that uses patterns of visible and ultraviolet light to dictate which of two monomers are polymerized to form a solid material. Different patterns of light provide the spatial control necessary to yield multi-material parts. The work was published Feb. 15 in the journal *Nature Communications*.

"As amazing as 3D printing is, in many cases it only offers one color with which to paint," says UW-Madison Professor of Chemistry A.J. Boydston, who led the recent work with his graduate student Johanna Schwartz. "The field needs a full color palette."

Boydston and Schwartz knew that improved printing materials required a chemical approach to complement engineering advances.

## Developable mechanisms can reside inside the surface of a structure

It took just over 10 years, but real science has finally caught up to the science fiction of Iron Man's transforming exoskeleton suit.

In a paper published today in *Science Robotics*, engineers at Brigham Young University detail new technology that allows them to build complex mechanisms into the exterior of a structure without taking up any actual space below the surface.

This new class of mechanisms, called "developable mechanisms," get their name from developable surfaces, or materials that can take on 3-D shapes from flat conformations without tearing or

stretching, like a sheet of paper or metal. They reside in a curved surface (like, say, the arms of Iron Man's suit) and can transform or morph when deployed to serve unique functions. When not in use, they can fold back into the surface of the structure seamlessly.

"These new discoveries make it possible to build complex machines that integrate with surfaces to be very compact, but can deploy and do complex tasks," said researcher Larry Howell, professor of mechanical engineering at BYU. "It opens up a whole new world of potential devices that have more functions, but are still very compact."

## Water-resistant electronic skin with self-healing abilities created



Along developed riverbanks, physical barriers can help contain flooding and combat erosion. In arid regions, check dams can help retain soil after rainfall and restore damaged landscapes. In construction projects, metal plates can provide support for excavations, retaining walls on slopes, or permanent foundations. All of these applications can be addressed with the use of sheet piles, elements folded from flat material and driven vertically into the ground to form walls and stabilize soil. Proper soil stabilization is key to sustainable land management in industries such as construction, mining, and agriculture; and land degradation, the loss of ecosystem services from a given terrain, is a driver of climate change and is estimated to cost up to \$10 trillion annually.

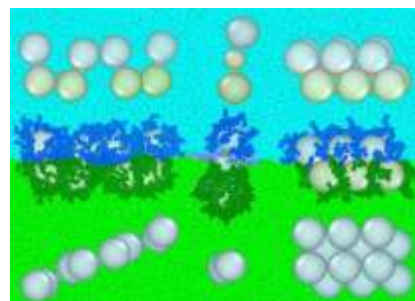
With this motivation, a team of roboticists at Harvard's Wyss Institute for Biologically Inspired Engineering has developed a robot that can autonomously drive interlocking steel sheet piles into soil. The structures that it builds could function as retaining walls or check dams for erosion control. The study will be presented at the upcoming 2019 IEEE International Conference on Robotics and Automation.

Conventional sheet pile driving processes are extremely energy intensive. Only a fraction of the weight of typical heavy machinery is used for applying downward force. The Wyss team's "Romu" robot, on the other hand, is able to leverage its

own weight to drive sheet piles into the ground. This is made possible by each of its four wheels being coupled to a separate linear actuator, which also allows it to adapt to uneven terrain and ensure that piles are driven vertically. From a raised position, Romu grips a sheet pile and then lowers its chassis, pressing the pile into the soil with the help of an on-board vibratory hammer. By gripping the pile again at a higher position and repeating this process, the robot can drive a pile much taller than its own range of vertical motion. After driving a pile to sufficient depth, Romu advances and installs the next pile such that it interlocks with the previous one, thereby forming a continuous wall. Once it has used all of the piles it carries, it may return to a supply cache to restock.

The study grew out of previous work at the Wyss Institute on teams or swarms of robots for construction applications. In work inspired by mound-building termites, Core Faculty member Radhika Nagpal and Senior Research Scientist Justin Werfel designed an autonomous robotic construction crew called TERMES, whose members worked together to build complex structures from specialized bricks. Further work by Werfel and researcher Nathan Melenbrink explored strut-climbing robots capable of building cantilevering truss structures, addressing applications like bridges. However, neither of these studies addressed the challenge of anchoring structures to the ground. The Romu project began as an exploration of methods for automated site preparation and installation of foundations for the earlier systems to build on; as it developed, the team determined that such interventions could also be directly applicable to land restoration tasks in remote environments.

## Layered liquids arrange nanoparticles into useful configurations



Materials scientists at Duke University have theorized a new "oil-and-vinegar" approach to engineering self-assembling materials of unusual architectures made out of spherical nanoparticles. The resulting structures could prove useful to applications in optics, plasmonics, electronics and multi-stage chemical catalysis.

The novel approach appeared online on March 25 in the journal *ACS Nano*.

Left to their own tendencies, a system of suspended spherical nanoparticles designed to clump together will try to maximize their points of contact by packing themselves as tightly as possible. This results in the formation of either random clusters or a three-dimensional, crystalline structure.

But materials scientists often want to build more open structures of lower dimensions, such as strings or sheets, to take advantage of certain phenomena that can occur in the spaces between different types of particles. And they're always on the lookout for clever ways to precisely control the sizes and placements of those spaces and particles.

In the new study, Gaurav Arya, associate professor of mechanical engineering and materials science at Duke, proposes a method that takes advantage of the layers formed by liquids that, like a bottle of vinaigrette left on the shelf for too long, refuse to mix together.





International  
**JOURNAL of  
SEWC**  
— Structural Engineers World Congress —